Universidade de São Paulo
Instituto de Biociências

Priscila Pires Bittencourt

Influência da disponibilidade hídrica sobre o comportamento fotossintético de *Portulaca oleracea* L.

Influence of water availability on the photosynthetic behavior of *Portulaca oleracea* L.

São Paulo
2018

Priscila Pires Bittencourt

Influência da disponibilidade hídrica sobre o comportamento fotossintético de *Portulaca oleracea* L.

Influence of water availability on the photosynthetic behavior of *Portulaca oleracea* L.

Dissertação apresentada ao Instituto de Biociências da Universidade de São Paulo, para a obtenção de título de Mestre em Ciências, na área de Botânica.
Orientador: Dr. Luciano Freschi

São Paulo
2018

Ficha Catalográfica

Bittencourt, Priscila Pires
Influência da disponibilidade hídrica sobre o comportamento fotossintético de *Portulaca oleracea* L.

Número de páginas: 53
Dissertação (Mestrado em Ciências) – Programa de Pós-Graduação em Botânica, Departamento de Botânica, Instituto de Biociências, Universidade de São Paulo, São Paulo, 2018.

1.Eficiência no uso da água. 2.Estresse hídrico. 3.Fotossíntese. 4.Metabolismo ácido das Crassuláceas. 5.*Portulaca*. Universidade de São Paulo. Instituto de Biociências. Departamento de Botânica.

Comissão Julgadora

_____ _____

Prof(a). Dr(a). Prof(a). Dr(a).

_____

Prof. Dr. Luciano Freschi
Orientador

AGRADECIMENTOS

Ao Departamento de Botânica do Instituto de Biociências da Universidade de São Paulo pelo apoio estrutural e ao CNPq pelo suporte acadêmico e financeiro sem o qual não seria possível realizar este projeto.

Ao Luciano Freschi, pela dedicação, empenho, paciência, ensinamentos, apoio e confiança. Pela orientação e toda troca de experiências.

Ao Marcos Buckeridge, Viviane Lopes, Fungyi Chow, Marilia Gaspar por disponibilizarem equipamentos importantes para realizção deste trabalho. Ao Diego Demarco pela colaboração na parte anatômica. Ao apoio técnico que facilitou e permitiu a realização desse trabalho, Aline Bertinatto, pela troca de experiência, auxílios e toda ajuda durante esses anos. Ao William, pelas boas risadas, apoio, conversas e amizade. A Ana Maria, pelo cuidado e atenção.

Aos companheiros de caminhada da fisiologia vegetal Ricardo Grilo Bianchetti por todo aprendizado, inspiração, conselhos e amizade construída. Ao Frederico, pela parceria, por todas as horas, carinho e apoio. Ao Filipe e o Bruno Gobara, pelas experiências compartilhadas e amizade. Ao Perdigão, pelas conversas, recepção e as boas histórias. Aos amigos do Laboratório de Fisiologia do Desenvolvimento Vegetal: Alejandra, Ana Z, Antônio, Auri, Carol, Marcos Marchesi, Paulo, Rafael, Renata, Valéria, que tornaram os dias e o trabalho melhor.

Aos amigos botânicos, Paulo e Gislaine. À Andressa e Pâmela, pelas boas risadas e conversas, apoio, carinho e amizade contruída. Ao Cadu, pela troca de experiência e construção dessa caminhada. À Leyde, pela paciência, companhia diária, cuidado, preocupação e consideração, à todos os nossos momentos e amizade contruída, em conjunto do Deni, por todas as risadas, bons cafés, filmes, carinho e zelo.

Aos amigos de vida, Bhetynna, Diego, Jéssica Pereira, João Pedro, Michelle Noronha. À Sara Sangi e Marcilio Zanetti, por todo apoio, conversas, auxílio, suporte, amigos e companheiros de luta e reclamações diárias, por permanecer e estar, mesmo na distância. À Marilia Romanha, pela presença, conforto, cuidado e carinho, ao auxílio, incentivo, amizade e equilíbrio. Ao Caíque, pelas boas risadas, amizade e experiências computacionais. À Pollyanna, pela amizade, inspiração, conversas e apoio mútuo, por estar e se fazer presente independente da situação.

Aos meus pais, Wilson e Fabíola pelo apoio, amor e carinho. Por confiar em mim e fazer dessa jornada mais confortável possível. Por nunca desistir e me inspirar, sempre sendo meus exemplos de luta, força e caminhada. À minha irmã, Poliana, por todo companherismo, apoio e amizade, por ter trazido minha sobrinha, Marina, mais nova e maior integrante dessa família.

À Deus por todo cuidado e zelo nessa caminhada, tornando-a mais confortável e possível.

Por todos aqueles que contribuíram, direta ou indiretamente, para realização dessa dissertação, minha formação pessoal e profissional.

Obrigada!

INDEX

RESUMO

BITTENCOURT, Priscila Pires. Influência da disponibilidade hídrica sobre o comportamento fotossintético de *Portulaca oleracea* L. 2018. 53f. Dissertação (Mestrado em Ciências – Área Botânica) – Instituto de Biociências, Universidade de São Paulo, São Paulo, 2018.

O metabolismo ácido das crassuláceas (CAM) e a via C_4 são adaptações fotossintéticas que melhoram significativamente a eficiência no uso da água (WUE). Esses dois mecanismos concentradores de CO_2 (CCMs) compartilham semelhanças, incluindo a pré-fixação de CO_2 na forma de ácidos orgânicos através da atividade da enzima fosfo*enol*piruvato carboxilase (PEPC) e a subsequente descarboxilação desses ácidos próximos ao sítio ativo da Rubisco. A ocorrência simultânea de ambos os CCMs no mesmo tecido é vista como bioquimicamente conflitante; no entanto, a existência de espécies de *Portulaca* capazes de alternar entre as vias C_4 e CAM numa mesma folha desafia essa potencial incompatibilidade. Ao monitorar as características anatômicas, os parâmetros fotossintéticos, o acúmulo noturno de ácidos e a abundância de transcritos de genes relacionados aos comportamentos C_4 e CAM, o presente estudo buscou caracterizar as mudanças induzidas pela seca na expressão do CAM em tecidos foliares e caulinares de *Portulaca oleracea*. Enquanto a ocorrência do CAM nas folhas parece ocorrer de modo totalmente facultativo, tanto fatores ontogenéticos quanto ambientais parecem controlar a expressão desse comportamento fotossintético nos caules. Os dados revelaram que, dependendo das condições ambientais e da idade das plantas, os caules de *P. oleracea* podem realizar C_3 ou CAM, mas não a fotossíntese C_4. As análises de trocas gasosas e de fluorescência da clorofila *a* nas folhas das plantas submetidas à seca sugerem que a descarboxilação diurna dos ácidos orgânicos acumulados durante a noite forneceria CO_2 à Rubisco em níveis suficientes para manter a integridade e funcionamento do aparato fotossintetizante mesmo após exposição prolongada à seca. Em geral, nenhuma alteração anatômica marcante foi observada nas folhas ou caules durante a indução do CAM, sugerindo que as reprogramações da expressão gênica e do metabolismo respondem pela maior parte das mudanças associadas à transição de C_4 para CAM e de C_3 para CAM nas folhas e caules, respectivamente. Dados de expressão gênica também indicaram que a transição entre as vias C_3 e CAM nos caules requer alterações no perfil transcricional de um conjunto mais numeroso de genes relacionados aos CCMs do que a transição de C_4 para CAM nos tecidos foliares. Em conjunto, as dados obtidos revelam uma notável plasticidade fotossintética em *P. oleracea* e fornecem pistas importantes sobre os mecanismos responsáveis pela compatibilidade entre as vias C_4 e CAM nesta espécie vegetal.

Palavras-Chave: Eficiência no uso da água. Estresse hídrico. Fotossíntese. Metabolismo ácido das Crassuláceas. *Portulaca*.

ABSTRACT

BITTENCOURT, Priscila Pires. Influence of water availability on the photosynthetic behavior of *Portulaca oleracea* L. 2018. 53p. Thesis (Master in Science – Botany) – Bioscience Institute, University of Sao Paulo, Sao Paulo, 2018.

Crassulacean acid metabolism (CAM) and the C_4 pathway are photosynthetic adaptations that significantly improve plant water use efficiency (WUE). These two CO_2-concentrating mechanisms (CCMs) share many similarities, including the pre-fixation of CO_2 as organic acids via phospho*enol*pyruvate carboxylase (PEPC) and the subsequent decarboxylation of these acids near the active site of Rubisco. The simultaneous occurrence of both CCMs in the same tissues has long been regarded as biochemically conflicting; however, the existence of *Portulaca* species that can switch between C_4 and CAM pathways within a single leaf challenges this assumption. By monitoring anatomical traits, photosynthetic parameters, nocturnal acid accumulation and transcript abundance of C_4- and CAM-related genes, this study aimed to characterize the drought-induced changes in CAM expression in both leaf and stem tissues of *Portulaca oleracea*. CAM was shown to be expressed in an entirely facultative fashion in leaves whereas both ontogenetic and environmental cues seem to control CAM induction in the stem tissues. Data revealed that depending on the environmental conditions and plant age, *P. oleracea* stems can perform either C_3 or CAM, but not C_4 photosynthesis. Gas exchange and chlorophyll *a* fluorescence analysis suggested that the daytime decarboxylation of the organic acids accumulated overnight in CAM-performing leaves supplied CO_2 to Rubisco behind closed stomata at sufficient levels to maintain the photosynthetic apparatus integrity and functioning even after prolonged drought exposure. Overall, no marked anatomical changes were observed in *P. oleracea* leaves or stems during the CAM induction, suggesting that gene expression and metabolism reprogramming may account for most of the C_4-to-CAM and C_3-to-CAM transition in leaves and stems, respectively. Gene expression data also indicated that the switch between C_3 and CAM pathways in the stems requires the transcriptional regulation of a more extensive set of CCM-related genes than the C_4-to-CAM transition in the leaves. Altogether, our findings reveal a remarkable photosynthetic plasticity in *P. oleracea* and provide important clues about the mechanisms behind the compatibility between the C_4 and CAM pathways in this plant species.

Key-words: Water use efficiency. Drought stress. Photosynthesis. Crassulacean acid metabolism. *Portulaca*.

1. Introduction

Photosynthesis in plants

Photosynthesis is arguably one the most important biochemical processes on the planet. It initiates in the thylakoid membrane of the chloroplasts with the conversion of light energy into chemical energy in the form of two energy-transporting molecules, ATP and NADPH. The energy stored in ATP and NADPH molecules is subsequently used in a series of reactions in the stroma known as the C_3 cycle, the Calvin-Benson cycle or the photosynthetic carbon reduction cycle (PCR cycle), which is responsible for the fixation and reduction of CO_2 into sugars. The cycle begins when CO_2 is combined with a five-carbon acceptor molecule, 1,5-ribulose bisphosphate (RuBP), generating an unstable six-carbon molecule that splits into two molecules of a three-carbon compound, 3-phosphoglycerate (3-PGA). This reaction is catalyzed by RuBP carboxylase/oxygenase (Rubisco), a key enzyme abundantly found in all photosynthetic organisms. Subsequent reactions in the Calvin cycle lead to the conversion of 3-PGA into trioses phosphate as well as the regeneration of RuBP (Whitney *et al.*, 2011; Raven and Beardall, 2016).

Importantly, Rubisco catalyzes either the carboxylation or oxygenation of RuBP depending upon the relative molecular concentration of carbon dioxide or oxygen near the enzyme active site. Under low CO_2 availability, Rubisco oxygenase activity is intensified resulting in the production of PGA and phosphoglycolate (PG), the latter being a toxic molecule capable of inhibiting photosynthesis. Whereas PGA can be recycled through the Calvin cycle, PG is converted to PGA via a coordinated series of chemical reactions in chloroplasts, peroxisomes and mitochondria (Bauwe *et al.*, 2010; Sage *et al.*, 2012). The formation and recycling of PG, known as photorespiration, can significantly limit carbon gain in plants performing C_3 photosynthesis, particularly under environmental conditions such as water deficit, when CO_2 concentration inside the leaves decline due to the reduced stomatal conductance. At current atmospheric levels of CO_2 and O_2, it is estimated that photorespiration dissipates about 25% of the organic carbon initially fixed in C_3 plants (Peterhansel and Maurino, 2011). Therefore, photorespiration is interpreted as wasteful process and is very likely a vestige of the high CO_2 and O_2 atmospheric concentrations (~1,000 ppm) under which the Rubisco-mediated CO_2 fixation initially evolved (~3.5 billion years ago) (Sage, 2004).

Over the last 40 million years ago (Mya) until the beginning of modern human era,

atmospheric levels of CO_2 have considerably declined (Zhang *et al.*, 2013) and this environmental change has been advocated as a major evolutive driver for terrestrial plants evolving innovative photosynthetic pathways capable of withstanding the atmospheric decline in CO_2 concentration. These adaptive traits are known as CO_2-concentrating mechanisms (CCMs), and in land plants primarily comprise the C_4 and the Crassulacean acid metabolism (CAM). C_4 and CAM plants evolved from C_3 ancestors, recruiting existing genes involved in anaplerotic functions to play photosynthesis-related roles (Sage, 2002; Edwards and Ogburn, 2012). Both photosynthetic behaviors independently evolved several times, with CAM occurring first whereas C_4 probably evolved more recently (Silvera *et al.*, 2010; Edwards and Ogburn, 2012).

C_4 photosynthesis

C_4 photosynthesis evolved independently more than 60 times in 19 different Angiosperm families (Sage *et al.*, 2011, 2014). The evolution of the C_4 metabolism involves a series of biochemical and metabolic modifications, including increased photosynthetic capacity, repositioning of the organelles, changes in enzymatic kinetics and regulatory properties, redistribution of enzymes within the tissues, among others (Sage *et al.*, 2011, 2012). Moreover, in the so-called dual-cell C_4 plants, the evolution of C_4 also involved relevant structural changes, including the development of a inner ring of bundle sheath cells (BSCs) around vascular tissues and an outer layer of mesophyll cells (MCs) in contact with the epidermis (*i.e.* Kranz anatomy) (Sage, 2004; Voznesenskaya *et al.*, 2010). However, relatively rare examples of single-cell C_4 species have also been found both in aquatic (e.g. *Hydrilla verticillata*, *Egeria densa*) and terrestrial environments (e.g. *Borszczowia aralocaspica*, *Bienertia cycloptera*), which are able to concentrate CO_2 at the active site of Rubisco due to a polarized distribution of the organelles within each photosynthetic cell (Sage, 2002; Voznesenskaya *et al.*, 2002; Edwards *et al.*, 2004).

In dual-cell C_4 plants, CO_2 is converted to bicarbonate (HCO_3^-) via carbonic anhydrase (CA) before being fixed by phospho*enol*pyruvate carboxylase (PEPC) in the MCs. The carboxylation catalyzed by PEPC consumes phospho*enol*pyruvate (PEP) and HCO_3^- to form oxaloacetate (OAA) and inorganic phosphate (Pi), and this reaction is facilitated by the high affinity of PEPC for CO_2 (~60 times higher than that of Rubisco) (Edwards *et al.*, 2004). The OAA formed is converted to a four-carbon acid (malate or aspartate), and these acids are transported to the BSCs, where they are decarboxylated via NAD(P) malic enzyme (NAD-ME and/or NADP-ME), and the CO_2 released is refixed by Rubisco, initiating the Calvin cycle. The pyruvate (Pyr)

formed during the decarboxylation process is transported to the chloroplast of MCs, where it becomes the substrate for the enzyme pyruvate orthophosphate dikinase (PPDK) to regenerate PEP, restarting the C_4 cycle (Fig. 1) (Voznesenskaya *et al.*, 2002; Sage, 2004).

This spatial separation between the sites of CO_2 pre-fixation via PEPC and the CO_2 assimilation site via Rubisco provided by the Kranz anatomy results in a higher concentration of CO_2 near the active site of Rubisco, thereby minimizing the occurrence of photorespiration and facilitating high rates of atmospheric CO_2 fixation in hot and moderately dry environmental conditions (Kraybill and Martin, 1996*;* Kanai and Edwards, 1999). In agreement, C_4 plants are predominantly found in tropical, subtropical and hot temperate regions (Edwards *et al.*, 2010).

In line with the multiple evolutive origins of C_4, considerable structural, metabolic and physiological diversity can be observed among C_4 plants. About 22 types of Kranz anatomy variants have already been described (Freitag and Stichler, 2000; Sage *et al.*, 2011; Kadereit *et al.*, 2013; Voznesenskaya *et al.*, 2017); the atriplicoid-type anatomy, which exhibits a complete sheath around the bundles, being the most commonly found (Sage *et al.*, 2011).

In terms of decarboxylation system, two major C_4 types have been described: the NADP-ME and the NAD-ME types. In the NADP-ME type, the OAA produced in the MCs is reduced to malate and transported to BSC chloroplasts, where the decarboxylation takes place releasing pyruvate. NADP-ME is the primary decarboxylation system in about 43 C_4 lineages, including all major high-productive monocot crops such as maize (*Zea mays*), sugarcane (*Saccharum* spp.) and sorghum (*Sorghum bicolor*) (Sage, 2004; Muhaidat *et al.*, 2007). Conversely, in the NAD-ME type, most OAA is transaminated to aspartate in the cytoplasm and transported to BSC mitochondria, where the decarboxylation takes place releasing pyruvate, which in turn is transaminated to alanine (Kanai R. and Edwards, 1999; Furbank, 2011) Species from 20 lineages, mostly eudicots, utilizes NAD-ME as the major decarboxylation system, including *Cleome* species (Brautigam *et al.*, 2011), *Amaranthus hypochondriacum* (Long *et al.*, 1994), among others. A third decarboxylation enzyme, the phospho*enol*pyruvate carboxykinase (PEPCK), is usually described as playing an accessory role rather than being the exclusive decarboxylation system in C_4 plants, therefore coexisting with either NADP-ME or NAD-ME enzymes (Muhaidat *et al.*, 2007; Bräutigam *et al.*, 2014; Wang *et al.*, 2014).

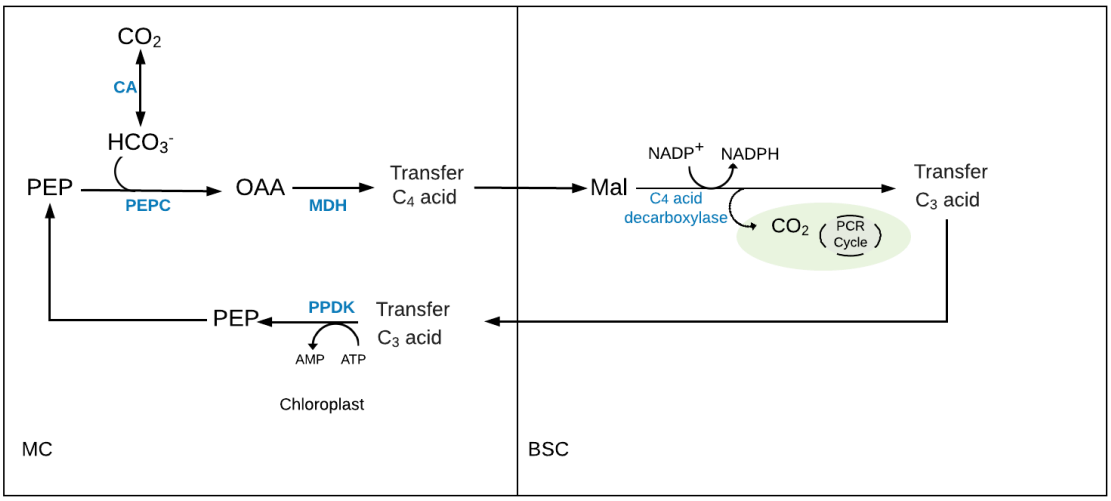

Figure 1: A simplified view of the C_4 pathway. In mesophyll cell (MC), CO_2 is converted to bicarbonate (HCO_3^-) by carbonic anhydrase (CA). HCO_3^- is then combined to phospho*enol*pyruvate (PEP) by PEP carboxylase (PEPC) to form oxaloacetate (OAA), which is converted into another 4-C organic acid (malate or aspartate) that is shuttled to bundle sheath cells (BSC). Decarboxylation of the 4-C organic acid in the BSC releases CO_2 that initiates the photosynthetic carbon reduction cycle (PCR cycle). The 3-C organic acid released from the decarboxylation is transferred to the MCs, where it is phosphorylated to PEP by pyruvate phosphate dikinase (PPDK).

Comparative studies performed in C_3 and C_4 species of *Flaveria* or *Cleome* revealed that virtually all enzymes required for the C_4 pathway are present in C_3 plants (Brautigam *et al.*, 2011). Therefore, increased attention has been devoted to understanding how these genes were recruited as such knowledge may significantly facilitate the current endeavors of engineering C_4 into C_3 species (Aubry *et al.*, 2011). Besides possessing both C_3 and C_4 species, the genus *Flaveria* also comprises some C_3–C_4 intermediate species, which have also been intensively studied as a means to develop hypotheses about the evolution and functioning of C_4 photosynthesis (McKown *et al.*, 2005; Vogan *et al.*, 2007).

Crassulacean acid metabolism (CAM)

CAM photosynthesis is particularly frequent among vascular plants inhabiting arid and semiarid environments, being found in approximately 16,800 species of 343 genera in 34 families, including angiosperms (monocotyledons and eudicots) as well as gymnosperms (Winter and Holtum, 2002; Silvera *et al.*, 2010). Several commercially important species, such as pineapple (*Ananas comosus*), agaves (*Agave* spp.), cactus (Cactaceae), and orchids (Orchidaceae), perform CAM photosynthesis and are recognized by their high water use efficiency (WUE) and remarkable

capacity to grow under relatively dry conditions (Cushman, 2001).

In CAM plants, stomata are typically open during the night, when CO_2 pre-fixation via PEPC generates OAA, which is converted to malate by cytosolic malate dehydrogenase (MDH) and subsequently accumulated overnight in the vacuole. During the day, malate is transported out of the vacuoles, where it is decarboxylated by a cytosolic NADP-ME or mitochondrial NAD-ME, producing CO_2 for subsequent fixation via Rubisco behind closed stomata (Cushman and Borland, 2002; Lüttge, 2004) (Fig. 2). Since the atmospheric CO_2 uptake in CAM plants usually takes place in moments of lower evaporative demand (i.e., nighttime, dawn and dusk), fewer water molecules are lost through transpiration per carbon molecule fixed, thus providing significantly higher WUE values than C_4, and particularly C_3 plants (Osborne and Sack, 2012).

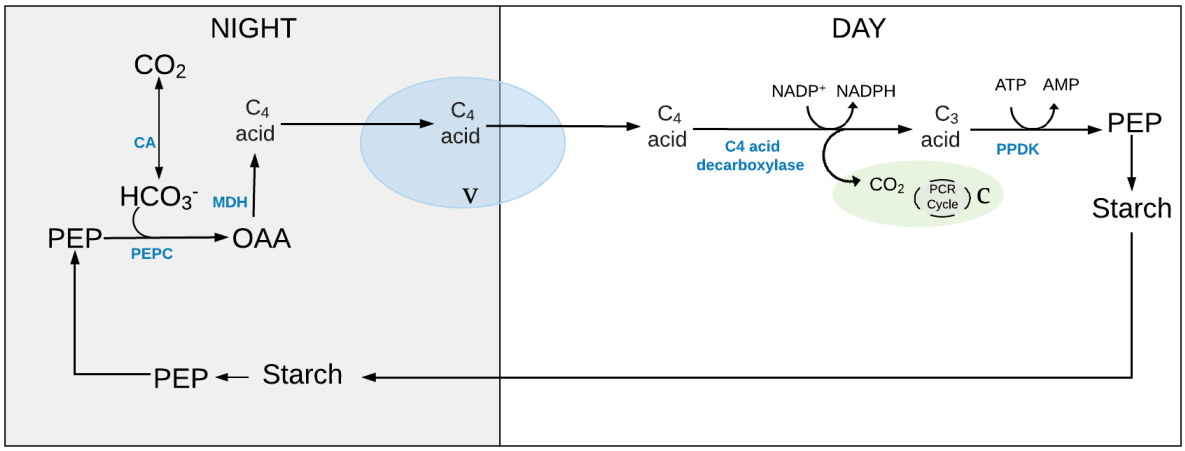

Figure 2: A simplified view of the CAM pathway. During the night, CO_2 is captured as bicarbonate (HCO_3^-) by phospho*enol*pyruvate carboxylase (PEPC) originating a C_4 acid (usually malate), which is accumulated overnight in the vacuole. During daytime, the C_4 acid leaves the vacuoles and is decarboxylated, releasing CO_2 to initiate the photosynthetic carbon reduction cycle (PCR cycle) in the chloroplast. The pyruvate (Pyr) released at the decarboxylation step is converted to triose phosphate and subsequently into starch. During the night, starch degradation contributes to the formation of PEP via pyruvate phosphate dikinase (PPDK) to reinitiate the CAM cycle. V, vacuole; C, chloroplast.

CAM photosynthesis may vary depending on the species and environmental conditions, operating in different modes according to the stomatal behavior and acid accumulation patterns (Cushman, 2001). In most CAM plants, stomata are open at night and closed during the day, and large amounts of organic acids are accumulated and consumed during the night and daytime, respectively. Representatives of this classic mode of CAM functioning include numerous species

belonging to Crassulaceae (e.g., *Kalanchoë daigremontiana*), Cactaceae (e.g., *Opuntia basilaris* and *Opuntia ficus-indica*), Bromeliaceae (e.g., *Bromelia humilis*) and Orchidaceae (e.g., *Schomburgkia humboldtiana*) families (Winter and Smith, 1996; Lüttge, 2004; Winter *et al.*, 2008).

In contrast, the so-called CAM cycling species exhibit daytime stomata opening as observed in C_3 plants while showing nocturnal acid accumulation derived from the refixation of nocturnally respired CO_2 (Herrera, 2009). When challenged with extreme drought conditions, CAM plants can also engage in a 'emergency mode' known as CAM idling, in which stomata remain closed 24 hours per day but a small diurnal fluctuation in organic acids remains due to respiratory CO_2 refixation (Lüttge, 2006; Freschi *et al.*, 2010). CAM idling mode does not allow additional carbon gain and consequently cannot support plant growth; however, it provides an efficient mechanism to recycle respiratory CO_2 behind closed stomata, thus minimizing water loss and potentially favoring a faster recovery in atmospheric CO_2 capture when environmental conditions become suitable to plant growth (Kraybill and Martin, 1996; Herrera, 2009).

Moreover, significant plasticity in CAM expression can be observed both within and between species. In recent years, CAM plasticity has been interpreted as a continuum trait, with constitutive plants exhibiting the lowest plasticity in CAM expression and facultative species at the opposite end. In adult constitutive plants, CAM photosynthesis is expressed even when environmental conditions are conducive to daytime CO_2 uptake. In contrast, the CAM behavior is an option rather than the mandatory carbon fixation mechanism in facultative species (Silvera *et al.*, 2010; Winter and Holtum, 2014). In facultative CAM plants, mature tissues can freely cycle between CAM and C_3 (or C_4) photosynthesis depending on the environmental conditions, frequently being promoted by drought and/or salinity (Winter and Holtum, 2014).

The induction of CAM in facultative species is one of the most complex metabolic adaptative responses against drought, involving extensive changes in gene expression, metabolic fluxes and stomatal behavior (Cushman and Borland, 2002). Recent studies have increasingly described facultative CAM species in plant families as diverse as Aizoaceae (*Mesembryanthemum crystallinum*), Bromeliaceae (*Guzmania monostachia*), Clusiaceae (*Clusia cylindrica*, *C. minor*, and *C. pratensis*), Talinaceae (*Talinum triangulare*), Piperaceae (*Peperomia scandens*), Portulacaceae (*Portulaca oleracea*), among others (Medina *et al.*, 1977; Koch and Kennedy, 1982; Herrera *et al.*, 1991; Holtum *et al.*, 2004; Winter *et al.*, 2008, 2009; Winter and Holtum, 2014).

Facultative CAM has been interpreted as particularly advantageous for annual species of semi-arid regions and/or environments characterized by a wet season followed by a period of drought (Lüttge, 2004). Under wet conditions, these plants can perform C_3 (or C_4) photosynthesis favoring fast and efficient growth, whereas a slow growth mode associated with reduced water loss can be maintained through CAM under water limiting conditions (Holtum *et al.*, 2018).

C_3-CAM facultative plants have received considerably more attention than C_4-CAM species most likely due to the more limited occurrence of the later. Currently, only six species have been shown to perform facultative C_4-CAM photosynthesis, all of them belonging to the genus *Portulaca* (*P. oleracea, P. grandiflora, P. australis, P. pilosa, P. cyclophylla* and *P. digyna*) (Koch and Kennedy, 1980, 1982; Ku *et al.*, 1981; Guralnick and Jackson, 2001; Guralnick *et al.*, 2002; Holtum *et al.*, 2017). More extensive screening is still required to evaluate whether other C_4 species may also be able to display CAM-like traits when challenged with limitations in the water supply or other environmental stresses.

C_4 and CAM: similarities and differences

C_4 and CAM behaviors share many similarities, including the pre-fixation of CO_2 as organic acids via PEPC and the subsequent decarboxylation of these acids near the active site of Rubisco. However, whereas the PEPC- and Rubisco-mediated carboxylation in C_4 plants take place in different compartments (MCs and BSCs, respectively), the separation between both carboxylation systems in CAM plants is rather temporal (i.e., PEPC at night and Rubisco during the day, both in the MCs). In both cases, an efficient accumulation of internal CO_2 is achieved, as CAM plants concentrate CO_2 in the dark in the form of acids whereas C_4 species concentrate CO_2 in the BSCs during the day.

Although the C_4 and CAM behaviors share similarities, the simultaneous occurrence of both CCMs in the same tissue has been regarded by some authors as biochemically conflicting (Sage, 2002). As described by Sage (2002), these two syndromes should be considered as incompatible because they present a differential regulation in the enzymatic activation of carboxylation and decarboxylation steps; metabolic transport dynamics and different structural arrangements for each syndrome (Kranz anatomy in C_4 and succulence in CAM). However, the existence of *Portulaca* species that can perform both C_4 and CAM photosynthesis within a single leaf indicates that both these photosynthetic adaptations can operate in the same tissues, probably

depending on additional layers of control of enzymes as well as transport and regulatory proteins. Therefore, investigating these species may provide important clues on how both syndromes can co-exist within a single individual, potentially opening up a window of opportunities for the future engineering of crops constitutive or facultatively expressing both CCMs.

Portulaca oleracea as a model system for investigating C_4/CAM compatibility

In the order Caryophyllales, eight families present C_4 photosynthesis (*i.e.* Aizoaceae, Amaranthaceae, Caryophyllaceae, Gisekiaceae, Molluginaceae, Nyctaginaceae, Polygonaceae, and Portulacaceae) and six families present CAM (*i.e.* Anacampserotaceae, Cactaceae, Didiereaceae, Montiaceae, Portulacaceae and Talinaceae) (Sage, 2004; Kluge and Ting, 1978; Richards, 1915; Winter, 1979; von Willert *et al*., 1992; Guralnick and Jackson, 2001; Koch and Kennedy, 1980; Martin and Zee, 1983). Both facultative and constitutive CAM have been reported in Montiaceae and Talinaceae (Herrera *et al.*, 1991; Winter and Holtum, 2011) whereas Portulacaceae contains the only known C_4-CAM species, all of which expressing CAM in a facultative fashion (Holtum *et al.*, 2017; Winter and Holtum, 2017)

Among the C_4-CAM *Portulaca* species, *P. oleracea* (commonly known as purslane) has received relatively more attention, showing drought-induced CAM expression in both leaves and stems (Mazen, 1996; Guralnick and Jackson, 2001; Guralnick *et al.*, 2002; Christin *et al.*, 2014; Winter and Holtum, 2014). This fast-growing herbaceous weed displays small succulent leaves with atriplicoid-type Kranz anatomy and large water storage cells (WSCs), exhibiting NAD-ME-type C_4 photosynthesis under well-watered conditions (Lara *et al.*, 2003, 2004; Voznesenskaya *et al.*, 2010; Ocampo *et al.*, 2013). Curiously, *P. oleracea* stems also present photosynthetically active cells, but lack Kranz anatomy traits, very likely performing C_3 photosynthesis under well-watered conditions (Kraybill and Martin, 1996; Voznesenskaya *et al.*, 2010). Therefore, this species seems to perform facultative C_4-CAM in the leaves and C_3-CAM in the stems, thereby representing a particularly interesting system for investigating the genetic, biochemical and physiological mechanisms behind such remarkable photosynthetic plasticity (Kraybill and Martin, 1996; Mazen, 1996; Lara *et al.*, 2003, 2004).

In one of the first studies on the occurrence of CAM behavior in this species, Kraybill and Martin (1996) found a significant nocturnal accumulation of titratable acidity under water deficit conditions. Distinct kinetic properties of PEPC in C_4- and CAM-performing *P. oleracea* were later

demonstrated, suggesting that specific PEPC isoforms would be expressed in each of these two photosynthetic behaviors (Mazen, 1996; 2000) In line with this, Christin *et al.* (2014) identified two *PPC* genes differentially expressed in well-watered and droughted *P. oleracea* plants.

Immunolocalization data obtained by using an antibody against maize PEPC, suggested that PEPC may be expressed both in MCs and WSCs of both well-watered and droughted plants (Guralnick *et al.*, 2002; Lara *et al.*, 2003, 2004). Moreover, Rubisco was shown to remain in the BSCs even after the drought-induced C_4-to-CAM transition, thereby implicating that an alternative model of CAM functioning may take place in *Portulaca* leaves. Based on this set of evidence, two distinct hypothetical models have been proposed for the C_4-CAM system in *Portulaca* leaves: (1) during CAM induction, acids accumulated overnight in both MCs and WSCs are shutlled to the BSCs for decarboxylation, which would caracterized an alternative, two-cell CAM system, herein addressed as a 'C_4-CAM hybrid' system (Lara *et al.*, 2003, 2004); and, (2) CAM could occur independently of the C_4 pathway, operating as a typical single-cell CAM system in MCs and WSCs relaying on very low Rubisco activity levels in those cells (Guralnick *et al.*, 2002). It is important to highlight that both these hypotheses still lack conclusive evidence; therefore, additional information is needed to clarify how a 'C_4-CAM hybrid' system can work in plants. Thus, *P. oleracea* offers us an opportunity to investigate in greater depth the biochemical, physiological, genetic and regulatory aspect associated with the occurrence of a 'C_4-CAM hybrid' system in plants, potentially enabling the future application of this knowledge for the genetic improvement of species of agronomic interest.

2. Objectives

General Objective

The overall aim of this Dissertation was to characterize the photosynthetic plasticity in *Portulaca oleracea* in response to changes in water availability.

Specific Objectives

To get insight into the general objective of this Dissertation, the following specific goals were set:

1) By monitoring photosynthetic parameters, chlorophyll *a* fluorescence, nocturnal acid accumulation and transcript abundance of C_4- and CAM-related genes, characterize the drought-induced changes in CAM expression in both leaf and stem tissues.

2) Investigate whether the drought-induced changes in CAM expression are associated with anatomical changes in both leaves and stems.

3. Material and methods

Plant material and experimental conditions

Plants of *Portulaca oleracea* subsp. *gigantea* were grown from seeds in 25-mL pots containing a 1:1 mixture of commercial substrate (Plantmax HT, Eucatex, São Paulo, Brazil) and vermiculite supplemented with 1 g L^{-1} of NPK 10:10:10, 4 g L^{-1} of dolomitic limestone ($MgCO_3$ + $CaCO_3$) and 2 g L^{-1} thermophosphate (Yoorin Master®, Yoorin Fertilizantes, Brazil). Plants were maintained in a growth chamber at a photosynthetic flux density (PFD) of about 350 μmol m^{-2} s^{-1}, 12h photoperiod, temperature of 27 ± 1ºC day and 22 ± 1ºC night and air humidity of 60% day and 70% night. Plants were watered daily before the start of the treatments.

After 20 days of initial growth, plants were separated into three experimental groups, each one submitted to a different watering regime as follows: (1) plants watered daily until field capacity (well-watered), (2) plants subjected to water withholding for 10 days followed by a period of 24 days under soil field capacity below 20% (droughted), (3) plants irrigated to field capacity after 34 days of drought (rewatered). Leaf and stem samples were harvested after 0 (D0), 10 (D1), 22 (D2) and 34 (D3) days of drought and after 4 (R1) and 8 (R2) days of rewatering treatments. All samples were harvested 1 h after the onset of illumination (dawn samples) and 1h before the end of the light period (dusk samples) in four biological replicates (each replicate was composed of a pool of whole stems or all full-expanded and non-senescent leaves of at least three plants).

Soil volumetric water content (SVWC) and tissue osmotic potential (Ψs)

Soil volumetric water content (SVWC) was continuously monitored (every 30 minutes) using Decagon soil moisture meter EC-5 coupled to the Em5b datalogger (Decagon Devices, Pullman, WA, USA). Osmotic potential (Ψ_s) of leaf and stem samples harvested at dawn (1h after the onset of illumination) were determined as described in Vieira *et al.* (2017). By using 20-mL disposable syringes, leaf and stem fragments were pressed to extract the sap, which was measured using a vapor pressure osmometer model VAPRO 5520 (Wescor, Logan, UT, USA). Osmolarity was measured in mmol kg^{-1} and transformed into MPa, using the Van't Hoff equation (Santa-Cruz

et al., 2002).

Leaf gas exchange and chlorophyll *a* fluorescence

Net CO_2 uptake (*A*, μmol CO_2 m^{-2} s^{-1}), stomatal conductance (*gs*, mol H_2O m^{-2} s^{-1}), transpiration rate (*E*, mmol m^{-2} s^{-1}) and the intercellular CO_2 concentration (C_i, μmol CO_2 mol^{-1}) were determined in the third fully expanded leaf (counting from the top) using with an infrared gas analyzer (Li 6400XT, Li-Color, Lincoln, USA). Measurements were performed between the 2nd and the 5th h after the onset of illumination, under controlled conditions of CO_2 concentration (380 ppm CO_2), photon flux density of 250 μmol m^{-2} s^{-1} and chamber temperature of 25ºC. Intrinsic water use efficiency (*iWUE*) was estimated as *A*/*gs*.

Chlorophyll *a* fluorescence was measured using a portable Pulse Amplitude Modulation fluorometer (PAM-2500, Walz, Germany). For the values of minimal (F_o) and maximal (F_m) fluorescence, leaves were dark-adapted for 30 min before a saturating pulse of light (3000 μmol photons m^{-2} s^{-1} for 1s). Dark-adapted PSII maximum quantum efficiency (F_v/F_m), effective quantum yield of the linear electron flow [Y(II)]; electron transport rate (ETR) were estimated according to Maxwell and Johnson (2000).

Titratable Acidity

For titratable acidity analysis, frozen leaf and stem samples (200 mg fresh weight - FW) were extracted in 1 mL 80 % (v/v) ethanol for 15 min at 80°C and the supernatants were recovered by centrifugation (5,000 *g*, 15 min). The pellets were re-extracted five times and all supernatants were combined before being titrated with 700 μM NaOH to pH 7.0 using phenolphthalein as indicator.

RNA isolation and quantitative RT-PCR analysis

Total RNA was extracted from ~100 mg FW of powdered leaf samples using ReliaPrep™ RNA Tissue Miniprep System (Promega) following the manufacturer's instructions for fibrous tissues. Complementary DNA (cDNA) was synthesized from 1 μg of total RNA using random primers and the SuperScript IV One-Step RT-PCR System (Invitrogen, USA), as recommended by the manufacturer. qRT-PCR reactions were performed in a StepOnePlus PCR Real-Time thermocycler (Applied Biosystems) in a final volume of 10 μl using 2X SYBR Green Master Mix

reagent (Thermo Fisher Scientific). Melting curves were checked for unspecific amplifications and primer dimerization. Absolute fluorescence data were analyzed using the LinRegPCR software package to obtain quantitation cycle (Cq) values and calculate primer efficiency. The relative gene expression was calculated applying the 2-ΔΔCT method (Livak and Schmittgen, 2001). Transcript abundances were normalized against the geometric mean of two reference genes, *CLATHRIN (PoCLAT)* and *UBIQUITIN-TRANSFERASE (PoUBQ)*. Primer sequences are listed in Table 1.

Table 1: Primer sequences.

Gene	**Primer sequences[1]**
PoUBQ (constitutive)	F: 5´- GATGGAAGTCGGACAGTGA - 3´/ R: 5´ - TGAAGCTGAGGGAAGTCG -3´
PoCLAT (constitutive)	F: 5´- GTAGTTCTGGGTCTGGTG - 3´/ R: 5´ - CGGCTTCTTCAATTAGGG - 3´
PoCA1	F: 5´- GAATTGGACACTCTCGCTG - 3´/ R: 5´ - GGAAATCTAGGATGTGAGAGG - 3´
PoCA3	F: 5´- GTGCCACATCAACGGATT - 3´/ R: 5´ - CTCACGAATGGGTATGTCAA - 3´
PoCA4	F: 5´- CAAGGCTAAGTACGTTGGAG - 3´/ R: 5´ - GCTCGCCAAAACCTTGT - 3´
PoPPC1	F: 5´- GTTCGTCGGTCTTTGCTTCAG - 3´/ R: 5´ -TCATCCTGTGGAGTTGGCTG - 3´
PoPPC2	F: 5´- CTCAGTGTCTTCTCCTAGAGG - 3´/ R: 5´ - GCGTCCTGCTTGTTGAATGC - 3´
PoMDH1	F: 5´- GGAGAATTGTGATGCCAGC - 3´/ R: 5´ - ATTTCCTCCCCATCAATCAAC - 3´
PoMDH3	F: 5´- ATCGTGAAGAACCTGGTC - 3´/ R: 5´ - GTCCACGTCAATCAGCTT - 3´
PoMDH4	F: 5´- GCTGAGGAGGAGACGAAA - 3´/ R: 5´ - ATGCTGACTTCCCTCAACC - 3´
PoMDH5	F: 5´- TGACGCATGGCTAAACAG - 3´/ R: 5´ - CGGCAGGAACGTTGTATG - 3´
PoNAD-ME1	F: 5´- AGAGGTATTGAGGGCGATG - 3´/ R: 5´ - AGCTCCCAAACCAATCCC - 3´
PoNAD-ME3	F: 5´- CAGAACTCCCGAAAGACAG - 3´/ R: 5´ - GCCCATCTTTTGCTTGCT - 3´
PoNADP-ME1	F: 5´- GAACAAACAACGAGGCAC - 3´/ R: 5´ - GGCTGTCCCCTGTATATCAT - 3´
PoNADP-ME2	F: 5´- GATGTTTACGGCGAGGAT - 3´/ R: 5´ - AGCAATCACAGAGGGAAC - 3´
PoPPDK1	F: 5´- TACTGGAATCTTGACGGCTC - 3´/ R: 5´ - CTAGATCGCCGCTAAGAG - 3´
PoASPT1	F: 5´- TGTTCTCGATTGTGTGCG - 3´/ R: 5´ - TCCAGTACCAGAGAGAGCC - 3´
PoASPT2	F: 5´- GAATTTGGGTGTTGGTGC - 3´/ R: 5´ - GATAAACATTGGACAGTGGT - 3´
PoASPT3	F: 5´- TTCTTGGCGTGTCTGAAG - 3´/ R: 5´ - TGAGGACGTATGGCTGAAG - 3´

[1]F: forward, R: reverse;

Anatomical analyses

Leaf and stem samples were fixed in FAA (formalin, acid acetic and ethanol 50% 9:1:1) for 24h and stocked in ethanol 70% (v/v), dehydrated, embedded in historesin (Leica®) and serial sectioned at 12 μm thickness on a Leica RM2145 rotary microtome (Leica Microsystems, Wetzlar, Germany). Transverse sections of the midrib of leaf and stem were stained with toluidine blue solution and analyzed by light microscopy (Leica Microsystems, Wetzlar, Germany).

Subsequently, starch grains were detected by adding Lugol`s reagent to the sections. To determine chloroplast distribution within the tissues, transversal leaf and stem cryosections were prepared using Leica KS34 cryomicrotome (Leica Microsystems) immediately analyzed using a UV epifluorescence microscope (DMLB; Leica) equipped with a Leica H3 filter (excitement at 420 nm and emission at 495 nm).

Statistical Analysis

Statistical analyses were performed using the JMP software package (SAS System for Windows, release 5.0.1a). Comparisons with $P \leq 0.05$ were considered statistically significant.

4. Results

Soil humidity and plant water status

After 10 days of water withholding soil volumetric water content (SVWC) was reduced to less than 25% of field capacity (Fig. 3A). Subsequent periodic supply of small volumes of water to the droughted plants (~10 mL per pot) maintained SVWC within 0 and 25% of field capacity during the rest of the drought treatment. Within the first 24h of rewatering, SVWC returned to values similar to those detected in the soil of the control group (Fig. 3A).

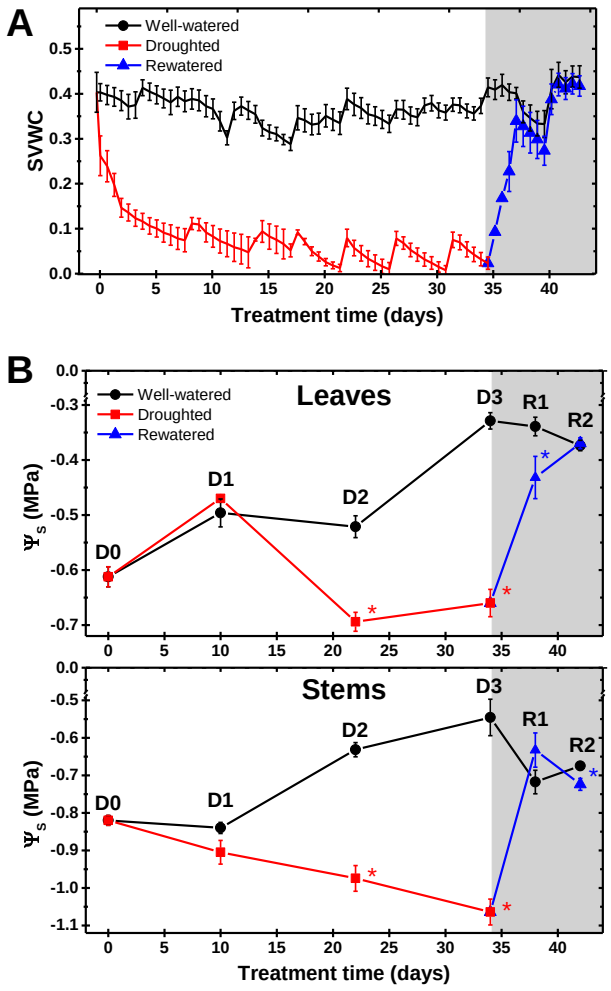

Figure 3. Soil humidity and plant water status. (A) Soil volumetric water content (SVWC) was continuously measured during the treatments. **(B)** Osmotic potential (*Ψs*) was measured in leaf and stem tissues of well-watered, droughted and rewatered plants. Gray area indicates the rewatering event. Data are means (±SE) of at least three replicates. In B, statistically significant differences compared with the well-watered sample were determined using Student's t-test: *P<0.05.

Although SVWC rapidly declined within the first 10 days of water withholding (D1), no significant differences in leaf and stem osmotic potential (Ψ_s) were observed between well-watered and droughted plants at this early stage of treatment (Fig. 3B). In contrast, significant reductions in both leaf and stem Ψ_s were detected later in the drought stress treatment (D2 and D3). Stem and leaf Ψ_s values rapidly increased upon rewatering (R1 and R2), achieving values similar to those observed in well-watered plants. An overall tendency of lower Ψ_s in the stem compared to the leaf tissues was observed regardless the watering treatment.

Drought treatment resulted in a significant reduction in plant growth, resulting in shorter and less branched plants than in the control group (Fig. 4). Plant growth was rapidly restored after rewatering (Fig. 4). In both well-watered and droughted plants, flowering started approximately 38 days after germination, corresponding to the D2 sampling point.

Figure 4: Visual phenotypes of well-watered, droughted and rewatered plants. Phenotypes of plants before the start of the drought treatment (D0), after 10, 22 and 34 days of drought treatment (D1, D2 and D3, respectively), and 4 and 8 days after rewatering (R1 and R2, respectively). In D1-D3, well-watered and droughted are shown on the left and the right, respectively. Bar = 07cm.

4.2. Leaf and stem anatomical traits

Microscopy analysis revealed that leaf and stem anatomy were not significantly altered in droughted *P. oleracea* plants compared to the well-watered ones, except for the reduction in the volume of the water storage cells (WSCs) in the leaves of droughted plants (Fig. 5). Regardless of the watering regime, typical atriplicoid-type leaf anatomy was observed, displaying several Kranz units, each one surrounding an individual vascular bundle. Stems were largely constituted by parenchyma cells and did not present typical Kranz-type anatomy traits.

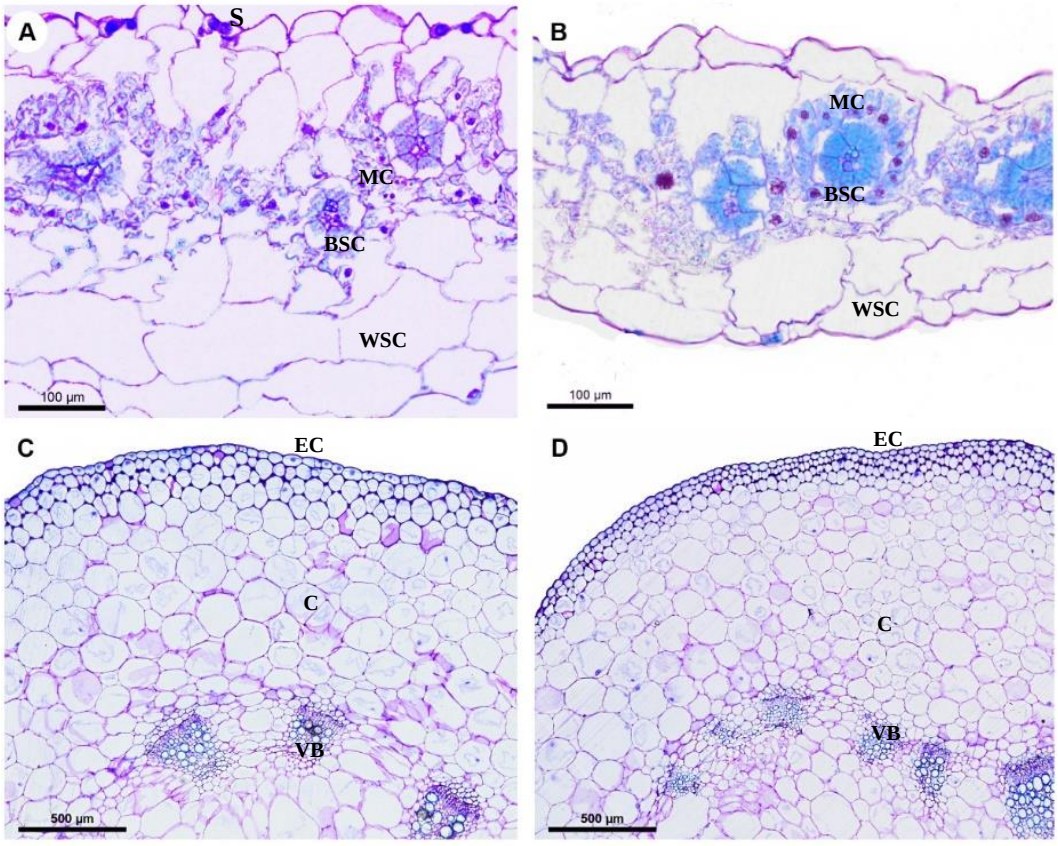

Figure 5: Cross-sections of *P. oleracea* leaves and stems. (**A**) Leaf section of well-watered plant. (**B**) Leaf section of droughted plant. (**C**) Stem section of well-watered plant. (**D**) Stem section of droughted plant. All samples were obtained from 54-day-old well-watered and droughted plants (D3 samples). EC, epidermal cell; BSC, bundle sheath cell; MC, mesophyll cell; WSC, water storage cell; S, stomata; C, cortex; VB, vascular bundle.

Bright field and fluorescence microscopy analysis revealed that chloroplasts are mainly located around the vascular bundles in both leaves and stems (Fig. 6A-G). In the leaves, these organelles were predominantly found the proximities of the bundles, throughout the mesophyll, forming multiple Kranz units. In the stem, chloroplasts form a well-delimited sheath in the inner cortex, also surrounding the vascular bundles (Fig. 6A-G). By revealing the distribution of the starch grains, Lugol staining confirmed the localization of the chloroplasts around the vascular bundles in both leaves and stems (Fig. 6I-J).

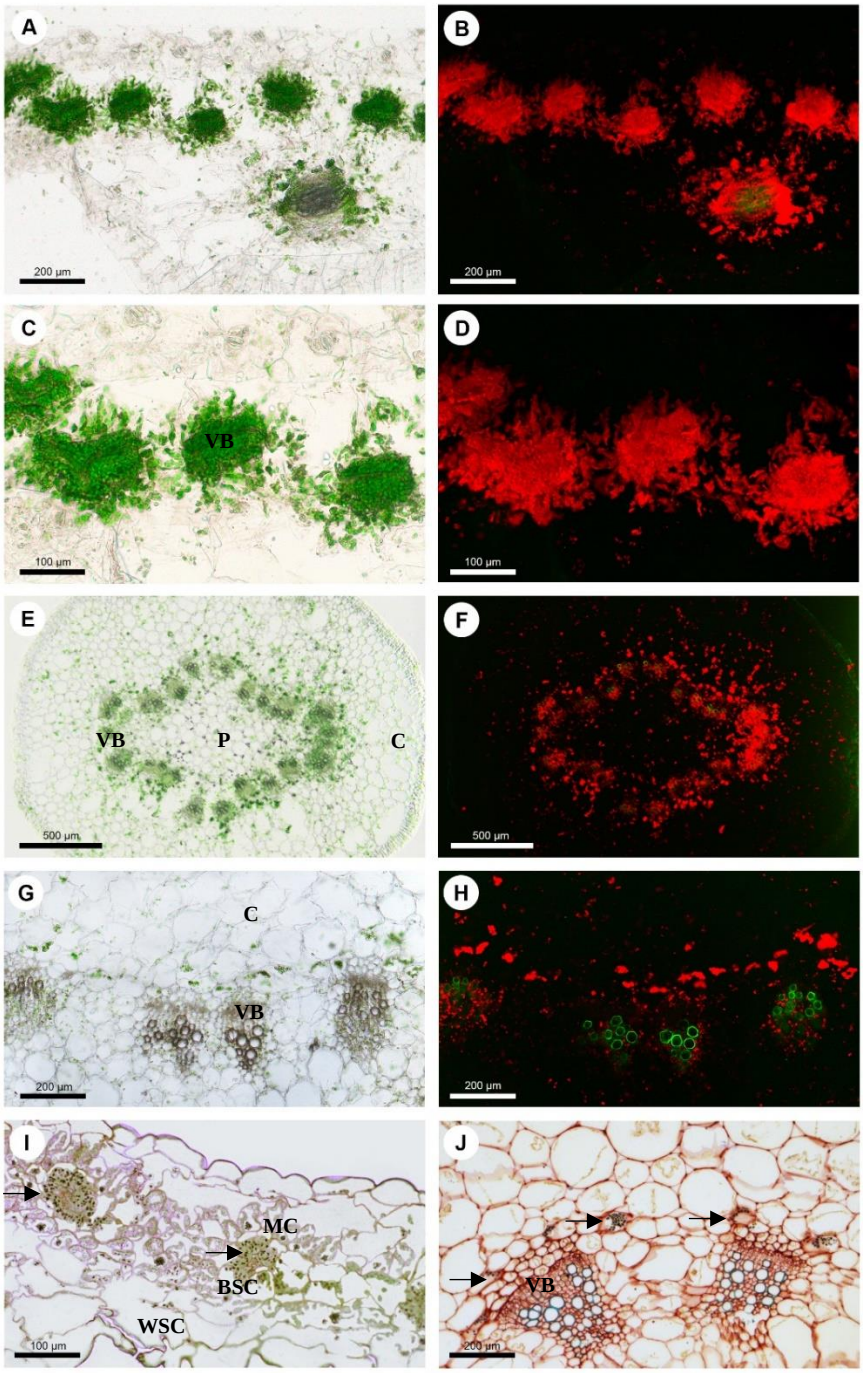

Figure 6: Distribution of chloroplasts in *P. oleracea* leaf and stem cross-sections. (**A-B**) Bright field and fluorescence microscopy of leaf sections. (**C-D**) Detail of A-B, showing the chloroplasts concentrated in the bundle sheath cells. (**E-F**) Bright field and fluorescence microscopy of stem sections. (**G-H**) Details of E-F, showing chloroplasts mainly present cells belonging to the inner cortex. (**I**) Lugol staining in leaf section. (**J**) Lugol staining in stem section. Red color in B, D, F and H represents chlorophyll autofluorescence under blue light. Arrows in I-J indicate the position of the starch reaction with Lugol (dark blue color). All samples were obtained from 54-day-old well-watered plants (D3 samples). BSC, bundle sheath cell; MC, mesophyll cell; WSC, water storage cell; C, cortex; VB, vascular bundle.

Impacts of water availability on gas exchange and chlorophyll fluorescence

Although no significant changes in both leaf and stem Ψ_s were observed within the first 10 days of water withholding (D1), drought plants exhibited a reduction of approximately 50% in stomatal conductance (g_s) and transpiration (E) compared to the well-watered individuals at this sampling point (Fig. 7). As no significant changes in net CO_2 uptake (A) were detected between control and droughted plants at D1, the water use efficiency (WUE) values exhibited by droughted plants were up to 2.7 higher than those observed in control plants (Fig. 7E). Prolonged drought treatment (i.e., D2 and D3 sampling points) led to a pronounced decline in A, g_s and E, achieving values close or below zero for these three gas exchange parameters (Fig. 7A-C). Net CO_2 uptake rapidly increased after rewatering, reaching values similar to control plants as soon as 4 days after rehydration (R1), remaining relatively unchanged thereafter. In contrast, g_s and E values gradually increased during the rewatering period, but did not achieve levels as high as those detected in well-watered plants even after 8 days of rewatering (R2).

The ratio between intra/extracellular CO_2 concentrations (C_i/C_a) in leaves of droughted and rewatered plants were maintained at similar or slightly lower levels than those detected in well-watered counterparts, except for the increment of approximately 50% in C_i/C_a observed in droughted plants at D3 sampling point (Fig. 7D). Neither drought nor rewatering treatments significantly altered chlorophyll *a* fluorescence parameters such as photochemical efficiency of the PSII (F_v/F_m), effective quantum yield of the linear electron flow [Y(II)] and electron transport rate (ETR). (Fig. 7F-H), suggesting that the marked impact of water availability on leaf gas exchange did not significantly affect the linear electron transport within the chloroplasts.

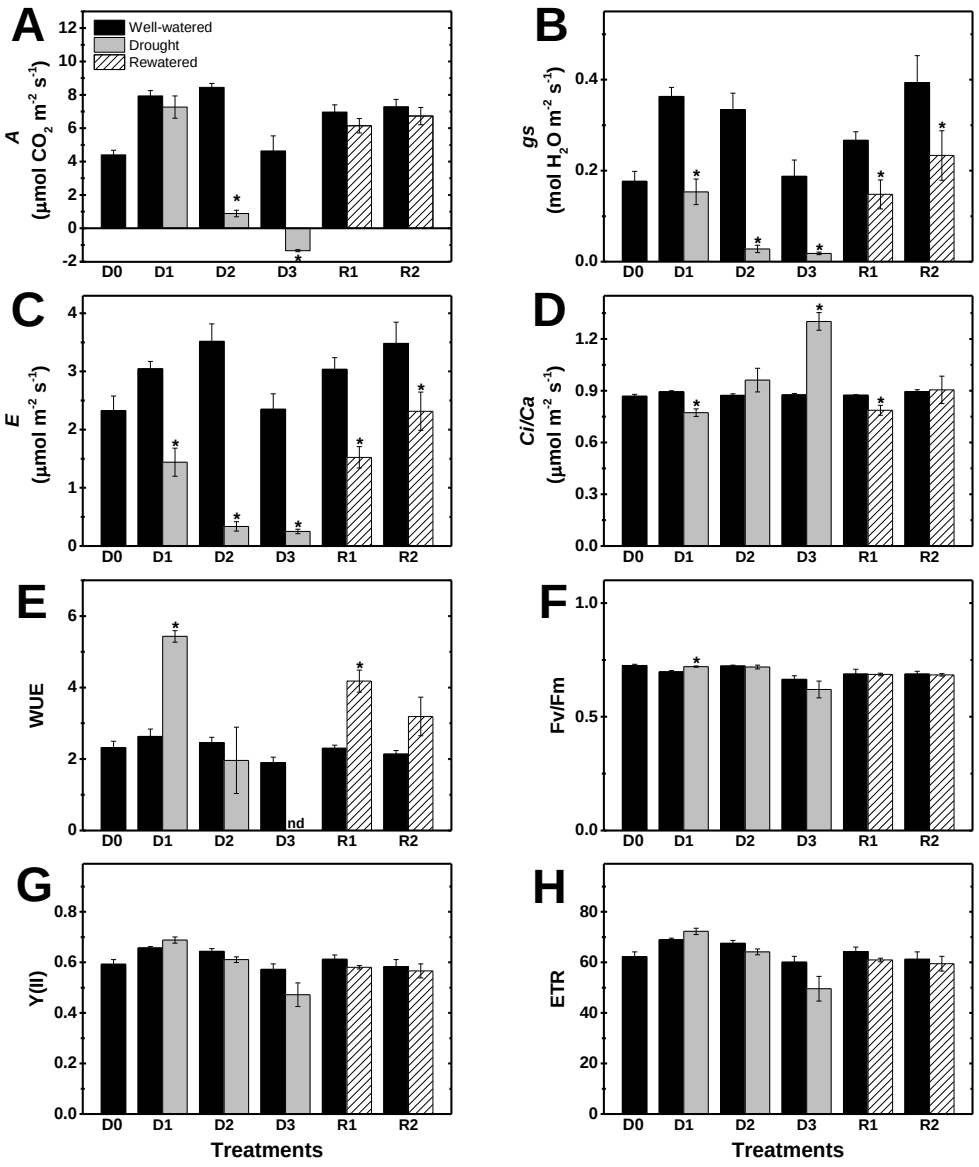

Figure 7: Leaf gas exchange and chlorophyll *a* fluorescence in response to changes in water availability. (**A**) Net CO_2 uptake (*A*). (**B**) Stomatal conductance (*gs*). (**C**) Transpiration (*E*). (**D**) Ratio between intra/extracellular CO_2 concentrations (C_i/C_a). (**E**) Water use efficiency (WUE). (**F**) Photochemical efficiency of the PSII (F_v/F_m). (**G**) Effective quantum yield of the linear electron flow [Y(II)]. (**H**) Electron transport rate (ETR). Data are means (±SE) of at least three biological replicates. Statistically significant differences compared with the well-watered samples were determined using Student's t-test: *P<0.05.

Impacts of water availability on nocturnal acid accumulation

As in other facultative CAM plants, the nocturnal acid accumulation has been widely used to monitor CAM expression in *P. oleracea* (Kraybill and Martin, 1996; Mazen, 2000; Lara *et al.*, 2003, 2004; Winter and Holtum, 2014). Here, the highest levels of leaf nocturnal acid

accumulation (ΔH^+) in droughted plants were detected at D1 and D2, declining in about 50% after prolonged drought (D3) (Fig. 8). Very limited ΔH^+ was observed at D0 and D1 sampling points in stems of both well-watered and droughted plants, indicating very low, if any, CAM expression in the stems at these sampling points. Conversely, stem ΔH^+ values in droughted samples were about 30 times higher than in well-watered counterparts at the D2 sampling point. As in the leaves, ΔH^+ in stems of droughted plants significantly declined after 34 days of drought treatment (D3) compared to samples harvested after 22 days of drought (D2). These findings indicate that 10 days of drought (D1) may be sufficient for inducing full CAM in the leaf tissues, whereas CAM expression in stems is achieved after more prolonged drought exposure, particularly at D2 sampling time. Prolonging the drought treatment (D3) negatively impacted nocturnal acid accumulation in both leaves and stems.

Interestingly, the maximum ΔH^+ values detected in stems of droughted plants were as high as those observed in the leaf tissues of the same plants (Fig. 8), suggesting a significant contribution of the stem tissues in storing CO_2 as organic acids overnight when *P. oleracea* plants are challenged by water-limiting conditions.

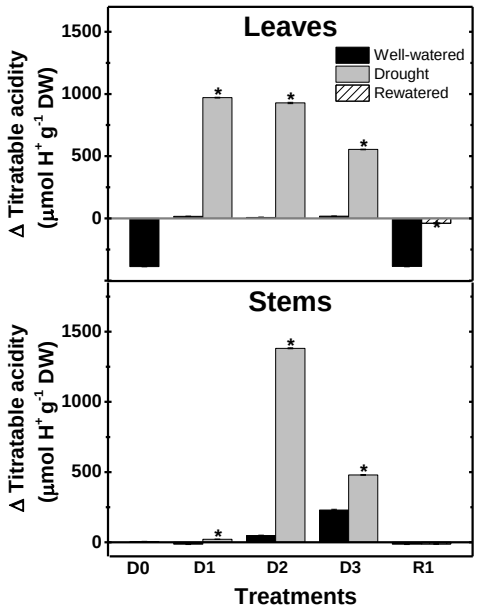

Figure 8: Nocturnal acid accumulation in response to changes in water availability. Titratable acidity at dusk and dawn was determined in both leaf and stem tissues of well-watered, droughted and rewatered plants. ΔH^+ indicates the dawn-dusk differences. Standard error of the dawn-dusk difference = $\sqrt{((\text{standard error}_{dawn})^2 + (\text{standard error}_{dusk})^2)}$. Data are means (±SE) of at least three biological replicates. Statistically significant differences compared with the well-watered samples were determined using Student's t-test: *P<0.05.

CAM was rapidly and fully reverted when the water supply is reestablished as indicated by the decline in both leaf and stem ΔH^+ to values close to zero within 4 days of rewatering (Fig. 8). Interestingly, however, distinct patterns of CAM expression were observed in well-watered leaves and stems. Under well-watered conditions, leaf ΔH^+ remained negative or close to zero all over the experiment, indicating that *P. oleracea* plants not challenged with drought can complete their life cycle without expressing CAM in the leaves. In contrast, positive ΔH^+ values were detected in stems of well-watered plants at both D2 and D3 sampling points, implicating that CAM expression in *P. oleracea* stems relies on both ontogenic and environmental regulation.

Transcriptional profiling of C_4- and CAM- related genes under contrasting water regimes

A set of candidate genes potentially involved in C_4 and CAM syndromes was selected from a large RNA-seq dataset recently generated for *P. oleracea* (unpublished data), and their relative transcript abundances were monitored during both the C_4-to-CAM and the CAM-to-C_4 switch in response to changes in water availability. Among the 18 genes were initially selected, five encoding enzymes involved in the carboxylation module (*PoCA1*, *PoCA3*, *PoCA4*, *PoPPC1* and *PoPPC2*), seven involved in the acid generation reactions (*PoMDH1*, *PoMDH3*, *PoMDH4*, *PoMDH5*, *PoASPT1*, *PoASPT2* and *PoASPT3*), four encoding malate decarboxylating enzymes (*PoNAD-ME1*, *PoNAD-ME3*, *PoNADP-ME1* and *PoNADP-ME2*), and two encoding pyruvate/orthophosphate dikinase (*PoPPDK1* and *PoPPDK2*), a key enzyme responsible for PEP regenerating.

The transcriptional profile of these genes in dawn and dusk leaf samples of *P. oleracea* performing either C_4 (D2, well-watered) or CAM (D2, droughted) revealed significantly higher *PoCA1*, *PoCA3*, *PoCA4*, *PoPPC1* and *PoASPT1* mRNA levels in C_4-performing plants and higher *PoPPC2*, *PoMDH1*, *PoMDH3*, *PoMDH4*, *PoMDH5*, *PoASPT2* , *PoASPT3* and *PoNADP-ME2* transcript abundance in CAM-performing individuals (Fig. 9). Overall, the highest change fold for the comparison between C_4- and CAM-performing samples were observed at dawn samples, except for the *PoPPC2* that peaked at dusk.

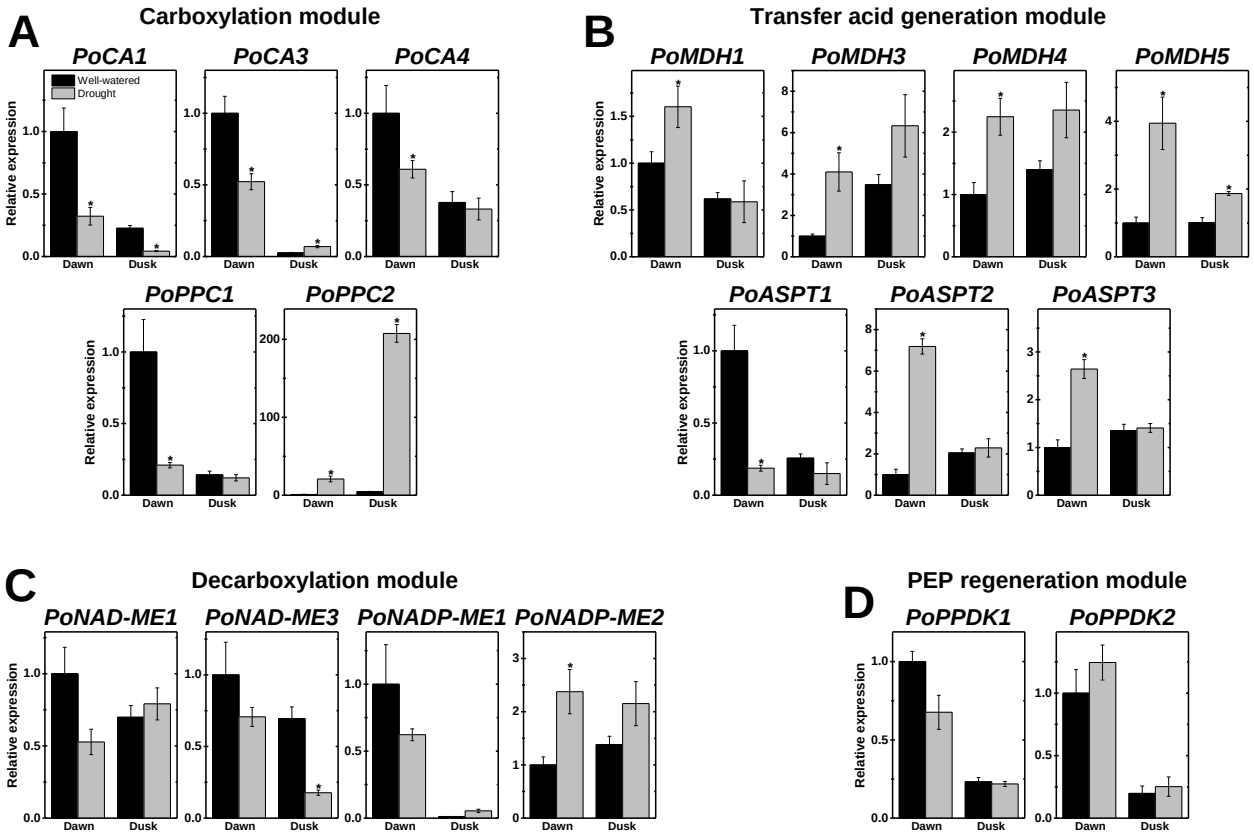

Figure 9: Transcriptional profile of C_4- and CAM-related genes. Transcript abundance of genes encoding major components of the carboxylation **(A)**, transfer acid generation **(B)**, decarboxylation **(C)** and phospho*enol*pyruvate (PEP) regeneration modules **(D)** was determined in leaves of well-watered and droughted plants (D2). Mean relative expression was normalized against well-watered samples harvested at dawn. Data are means (±SE) of at least three biological replicates. Statistically significant differences compared with the well-watered samples were determined using Student's t-test: *P<0.05. CA, carbonic anhydrase; PPC, phospho*enol*pyruvate carboxylase; MDH, malate dehydrogenase; ASPT, aspartate transaminase; NAD-ME, NAD-dependent malic enzyme; NADP-ME, NADP-dependent malic enzyme; PPDK, pyruvate/orthophosphate dikinase.

Significant differences in relative transcript ratios of genes encoding for the same enzyme were observed (Fig. 10). Among the CA-encoding genes, *PoCA1* and *PoCA3* transcripts were significantly more abundant than *PoCA4* regardless of the watering regime or the time of the day. *PoPPC1* was more abundantly expressed than *PoPPC2* under all conditions analyzed, except for the dusk samples of droughted plants. In all conditions, *PoMDH3* and *PoMDH4* were the least and most expressed MDH-encoding genes, respectively. *PoASPT2* was significantly more expressed than other ASPT genes under all conditions analyzed, exceeding in more than 60 times *PoASPT1* and *PoASPT3* in samples of droughted plants harvested at dawn. *PoPPDK1* was at least 50 times

more expressed than *PoPPDK2* under all conditions analyzed. Among ME-encoding genes, *PoNAD-ME1* and *PoNADP-ME1* were significantly more expressed than *PoNAD-ME2* and *PoNADP-ME2*. Interestingly, the transcript ratio of genes between *PoNAD-ME1* and *PoNADP-ME1* were relatively similar in samples harvested at dawn from either well-watered and droughted plants, thereby suggesting that both NAD-ME and NADP-ME may participate in malate decarboxylation in both C_4- and CAM-performing *P. oleracea* plants.

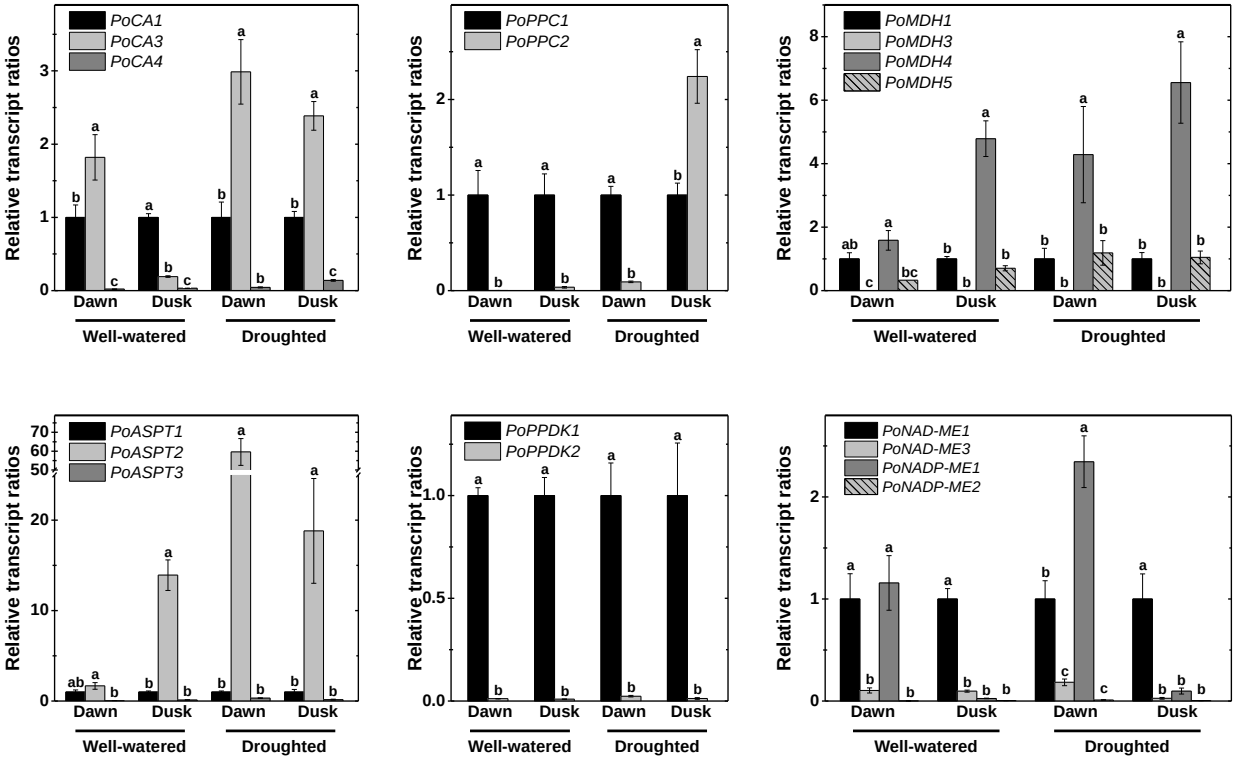

Figure 10: Relative transcript ratios of C_4- and CAM-related genes in *P. oleracea* leaves. Values represent means ± SD from at least three biological replicates and are expressed as relative transcript ratios between the distinct genes encoding for the same enzymes. Different letters indicate statistically significant differences (Tukey's test, $p < 0.05$) among the distinct genes encoding for the same enzyme at each sampling point. Transcript abundance was determined in leaves of well-watered and droughted plants (D2 sampling). *PoPCC2* mRNA levels were determined in dusk samples whereas all other gene expression data were generated using dawn samples. CA, carbonic anhydrase; PPC, phosphoenolpyruvate carboxylase; MDH, malate dehydrogenase; ASPT, aspartate transaminase; NAD-ME, NAD-dependent malic enzyme; NADP-ME, NADP-dependent malic enzyme; PPDK, pyruvate/orthophosphate dikinase.

Based on their differential expression in C_4- and CAM-performing samples (Fig. 9) and their transcript abundance ratio in relation to other genes encoding for the same enzymes (Fig. 10),

PoCA1, PoCA3, PoPPC1, PoPPC2, PoMDH4, PoMDH5, PoASPT1, PoASPT2, PoNAD-ME1, PoNADP-ME1 and *PoPPDK1* were selected for the next steps of this study.

Temporal and spatial transcriptional patterns of C_4- and CAM related genes

In both C_4 and CAM plants, the first carboxylation involves the interconversion of CO_2 and bicarbonate (HCO_3^-) via carbonic anhydrase (CA) and the subsequent addition of HCO_3^- to phospho*enol*pyruvate (PEP) via PEP carboxylase to form the four-carbon compound oxaloacetate (OAA) (Badger and Price, 1994). In *P. oleracea* leaves, *PoCA1* and *PoCA3* transcript levels were significantly reduced in response to water deficit, whereas rewatering promoted the accumulation of these transcripts (Fig. 11A). In contrast, *PoCA3* mRNA levels in the stems were approximately three times higher in droughted samples (D2 and D3) compared to well-watered ones. This drought-induced accumulation of *PoCA3* transcripts in stem tissues was completely reverted after rewatering (R1).

In line with previous findings (Christin *et al.*, 2014), two *PoPPC* with contrasting responses to water availability were identified. In leaves, *PoPPC1* and *PoPPC2* mRNA levels were significantly reduced and promoted in response to water limitation, respectively (Fig. 11B). The highest *PoPPC2* transcript abundance in leaves were detected in D2 sampling point more expressed in droughted than in well-watered samples. Whereas stem *PoPPC1* mRNA levels did not differ between droughted and well-watered samples, a progressive accumulation of *PoPPC2* transcripts was observed in stems from droughted plants. In both leaves and stems, rewatering up- and down-regulated *PoPPC1* and *PoPPC2*, respectively, to levels similar to those detected in well-watered plants. These findings support the view that *PoPPC1* and *PoPPC2* may encode the PEPCs responsible for OAA formation during C_4 and CAM photosynthesis, respectively. In line with this, *PoPPC1* mRNA levels peaked at dawn as expected for a PEPC isoform associated with the C_4 pathway, whereas *PoPPC2* peaked at dusk as commonly observed for other CAM-related PEPC isoforms (Christin *et al.*, 2014).

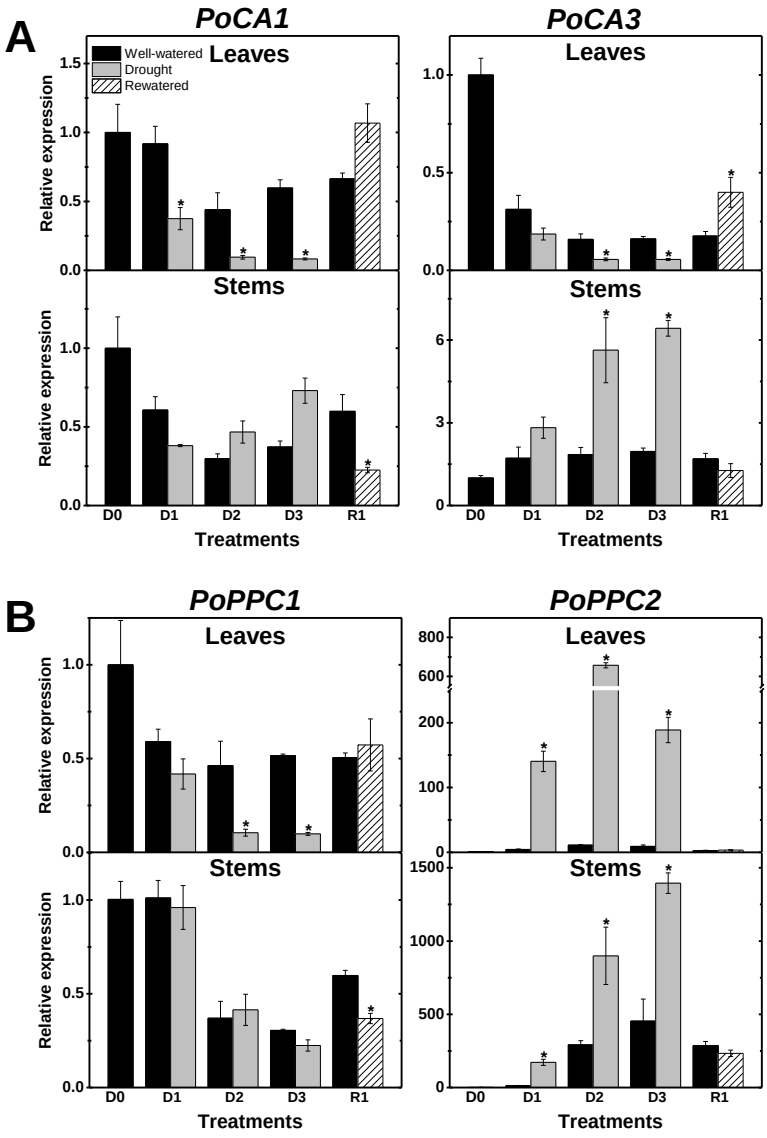

Figure 11: Transcript abundance of genes encoding key enzymes involved in the carboxylation module. (A) Carbonic anhydrase (CA)-encoding genes. **(B)** Phospho*enol*pyruvate carboxylase (PPC)-encoding genes. Transcript abundance was determined in leaves and stems of well-watered, droughted and rewatered plants. Mean relative expression was normalized against D0 samples. *PoCA1*, *PoCA3* and *PoPPC1* mRNA levels were determined in samples harvested at dawn. *PoPPC2* transcript abundance was determined in samples harvested at dusk. Data are means (±SE) of at least three biological replicates. Statistically significant differences compared with the well-watered samples were determined using Student's t-test: *P<0.05.

In CAM plants, the OAA formed via PEPC is converted to malate via malate dehydrogenase (MDH) and stored overnight in the vacuoles, whereas in C_4 plants the OAA is converted to malate via MDH or aspartate via aspartate aminotransferase (ASPT) before being

shuttled to the BSCs (Hatch *et al.*, 1988). After prolonged drought exposure (D2 and D3), *PoMDH4* and *PoMDH5* mRNA levels were significantly promoted in *P. oleracea* stems and leaves, respectively (Fig 12A). This suggests that these two MDH-encoding genes may be differentially recruited to convert OAA into malate in each of these two photosynthetically-active tissues (i.e., stems and leaves). After rewatering, *PoMDH4* and *PoMDH5* transcripts returned to levels similar to those observed in well-watered plants.

Drought differentially impacted *PoASPT1* and *PoASPT2* transcript accumulation, repressing the former and promoting the later in both leaves and stems (Fig. 12B). The overall drought-triggered changes in *PoASPT2* mRNA levels resembled those observed for *PoPPC2*. After rewatering, *PoASPT1* and *PoASPT2* mRNA in both leaves and stems returned to levels similar to those detected in well-watered samples. As observed for *PoPPC*s, the drought-induced downregulation of *PoASPT1* and upregulation of *PoASPT2* suggest that *PoASPT1* and *PoASPT2* are involved in C_4 and CAM photosynthesis, respectively.

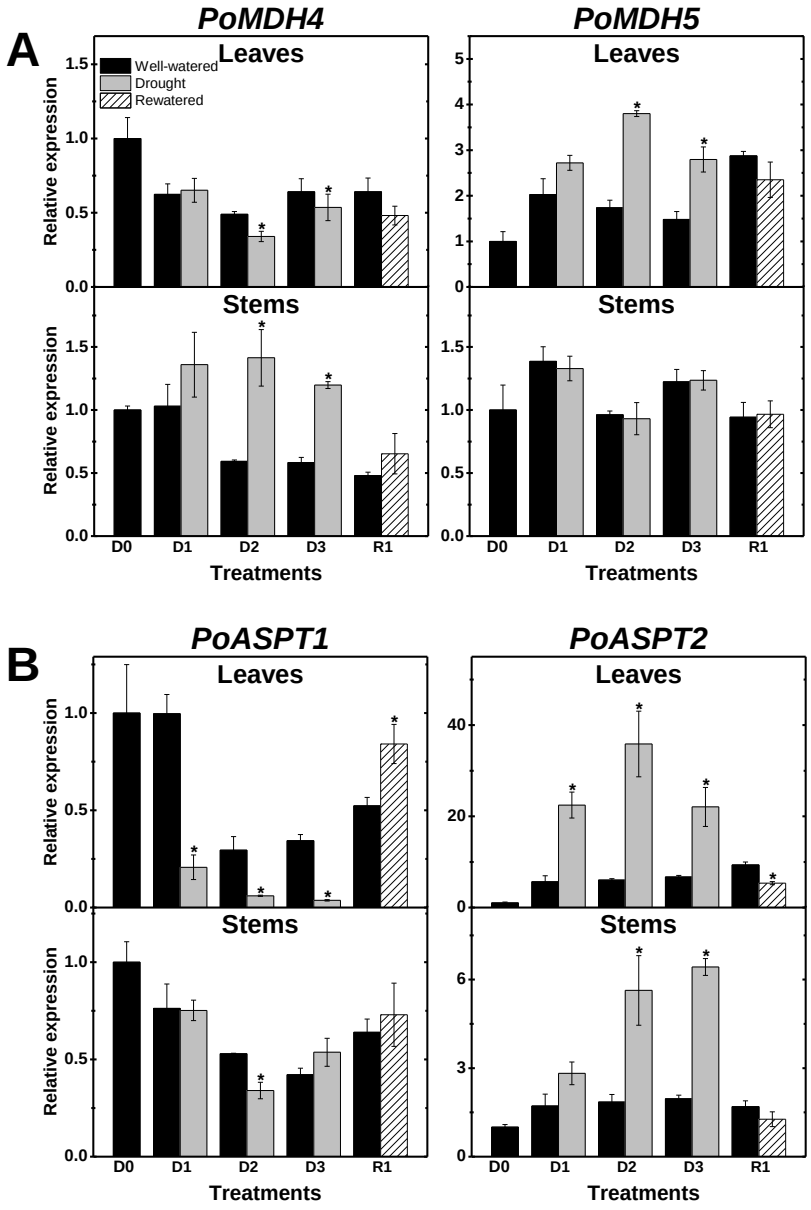

Figure 12: Transcript abundance of genes encoding key enzymes involved in the acid generation module. (A) Malate dehydrogenase (MDH)-encoding genes. **(B)** Aspartate transaminase (ASPT)-encoding genes. mRNA levels were determined in leaf and stem samples of well-watered, droughted and rewatered plants harvested at dawn. Mean relative expression was normalized against D0 samples. Data are means (±SE) of at least three biological replicates. Statistically significant differences compared with the well-watered samples were determined using Student's t-test: *P<0.05.

P. oleracea is regarded as a NAD-ME-type C_4 plant (Voznesenskaya *et al.*, 2010). Here, we demonstrate that *PoNAD-ME1* and *PoNADP-ME1* are the ME-encoding genes predominantly expressed in *P. oleracea* (Fig. 10). Interestingly, whereas *PoNAD-ME1* is expressed at similar

levels in dawn and dusk samples, *PoNADP-ME1* is predominantly expressed at dawn (Fig. 9). Overall, *PoNAD-ME1* and *PoNADP-ME1* exhibited similar gene expression patterns in responses to changes in water availability. In leaves, both these genes exhibited a decrease in relative expression as drought exposure was prolonged, followed by their upregulation to levels similar to the control as soon as four days after rewatering (R1) (Fig. 13). These results suggest a reduction in the NAD(P)-ME-dependent decarboxylation during the C_4-to-CAM transition in leaves. In contrast, an opposite trend was observed in stems as both *PoNAD-ME1* and *PoNADP-ME1* were clearly more expressed under drought than under well-watered or rewatered conditions. This indicates that, differently from the leaves, the CAM induction in stems presumably requires the upregulation of the NAD(P)-ME-dependent decarboxylation system.

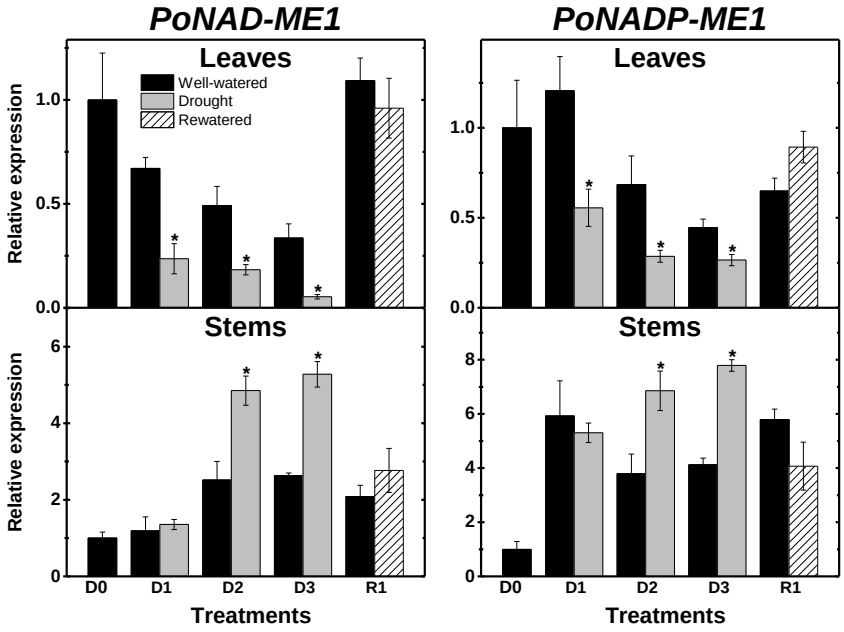

Figure 13: Transcript abundance of genes encoding key enzymes involved in the malate decarboxylation. mRNA levels were determined in leaf and stem samples of well-watered, droughted and rewatered plants harvested at dawn. Mean relative expression was normalized against D0 samples. Data are means (±SE) of at least three biological replicates. Statistically significant differences compared with the well-watered samples were determined using Student's t-test: *P<0.05. NAD-ME, NAD-dependent malic enzyme; NADP-ME, NADP-dependent malic enzyme.

The PPDK-mediated regeneration of PEP is a crucial step in both C_4 and CAM pathways (Chastain *et al.*, 2011). *PoPPDK1* was identified as the dominant PPDK-encoding genes in both C_4- and CAM-performing leaves of *P. oleracea* (Fig 10), and its transcript abundance in leaves

was progressively reduced in response to drought stress and rapidly increased in response to rewatering (Fig. 14). In contrast, *PoPPDK1* mRNA levels in stems of droughted or rewatered plants did not significantly differ from the well-watered plants at each sampling point. Therefore, the CAM induction in leaves was presumably accompanied by a reduction in PEP regeneration rates, whereas no changes in this metabolic step seem to be required for the CAM induction in stem tissues.

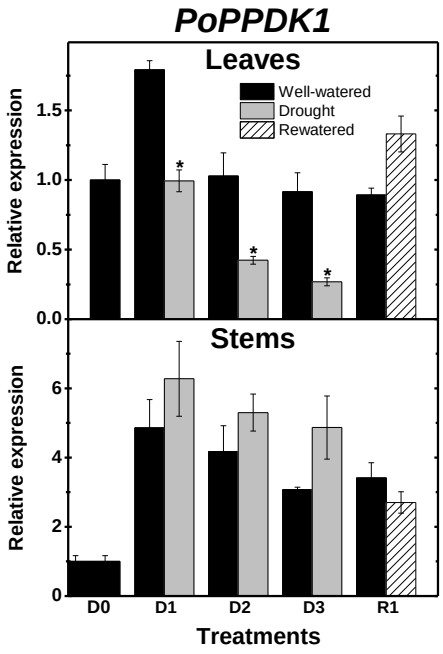

Figure 14: Transcript abundance of pyruvate/orthophosphate dikinase (PPDK)-encoding genes. mRNA levels were determined in leaf and stem samples of well-watered, droughted and rewatered plants harvested at dawn. Mean relative expression was normalized against D0 samples. Data are means (±SE) of at least three biological replicates. Statistically significant differences compared with the well-watered sample were determined using Student's t-test: *P<0.05.

Finally, the relative transcript ratios of C_4- and CAM-related genes were compared in leaves and stems of both well-watered (C_4-performing) and droughted (CAM-performing) plants. All CA-, NAD(P)-ME- and PPDK-encoding genes were significantly less expressed in stems than in leaves of both well-watered and droughted plants (Fig. 15). In contrast, both MDH-encoding genes analyzed were expressed at relatively similar levels in stems and leaves regardless of the watering regime.

Very interestingly, however, an evident pattern was observed for the PEPC- and ASPT-encoding genes analyzed. *PoPPC1* and *PoASPT1*, which were downregulated by drought and

consequently more closely related to C_4 photosynthesis (Figs. 11 and 12), were drastically less expressed in stems than in leaves (Fig. 15). In contrast, *PoPPC2* and *PoASPT2*, which were sharply upregulated by drought and consequently more closely related to CAM photosynthesis (Figs. 11 and 12), were expressed in stems at similar or even higher levels than those detected in the leaves (Fig. 15). Therefore, these findings suggest that C_4 photosynthesis in *P. oleracea* plants may be restricted to the leaves under well-watered conditions. In contrast, CAM expression in stems seems to be as high as those detected in the leaves under drought stress.

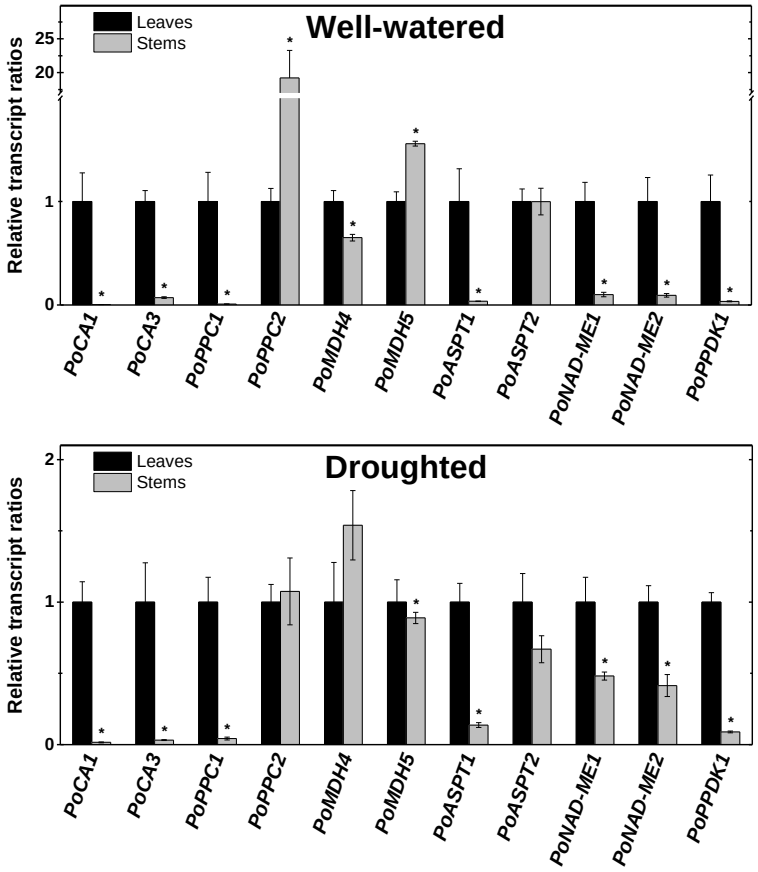

Figure 15: Relative transcript ratios of C_4- and CAM-related genes in leaves and stems. Values represent means ± SD from at least three biological replicates and are expressed as relative transcript ratios between the leaf and stem samples at the same experimental conditions. Different letters indicate statistically significant differences (Tukey's test, $p < 0.05$) between leaf and stem samples. Transcript abundance was determined in leaves and stems of well-watered and droughted plants (D2 sampling). *PoPCC2* mRNA levels were determined in dusk samples whereas all other gene expression data were determined in dawn samples. CA, carbonic anhydrase; PPC, phospho*enol*pyruvate carboxylase; MDH, malate dehydrogenase; ASPT, aspartate transaminase; NAD-ME, NAD-dependent malic enzyme; NADP-ME, NADP-dependent malic enzyme; PPDK, pyruvate/orthophosphate dikinase.

5. Discussion

P. oleracea is one of the few species capable of performing both C_4 and CAM within a single leaf, thereby representing a particularly convenient model system for dissecting how a single individual can express both these CCM syndromes depending on environmental and ontogenetic factors. As other facultative CAM species, water availability has been characterized as the predominant environmental factor controlling nocturnal acid accumulation in *P. oleracea* (Koch and Kennedy, 1980, 1982; Kraybill and Martin, 1996; Mazen, 2000; Guralnick and Jackson, 2001; Lara *et al.*, 2003, 2004). Here, we present physiological and gene expression evidence demonstrating that CAM expression in both leaves and stems of *P. oleracea* can be modulated in response to changes in water availability in a remarkably fast and fully reversible fashion. Monitoring the nighttime H^+ accumulation and several photosynthetic parameters revealed that leaves from both well-watered and rewatered *P. oleracea* plants predominantly perform C_4 whereas those exposed to drought clearly exhibit CAM photosynthesis. By comparing the transcript abundance of candidate genes in well-watered, droughted and rewatered plants, we found that *PoPPC1* and *PoASPT1* were predominantly expressed in C_4-performing individuals whereas *PoPPC2* and *PoASPT2* were most expressed in those engaged in CAM photosynthesis. Therefore, the differential recruitment of *PoPPC* and *PoASPT* genes into the C_4 and CAM pathways suggest that their encoding proteins may play a vital role in allowing both CCMs to occur within a single leaf. Moreover, these genes seem to represent excellent markers for monitoring the C_4-CAM transitions in this species.

Alongside with the changes in ΔH^+ and *PoPPC2* and *PoASPT2* expression patterns indicated that drought-induced CAM induction in leaves took place relatively faster in leaves than in stems. Whereas drought-induced CAM expression in stems was only detected at more advanced stages of the drought treatment (D2 and D3 samples), ΔH^+ as well as *PoPPC2* and *PoASPT2* transcript accumulation in the leaves were clearly induced by drought at all drought sampling points (D1, D2 and D3). Interestingly, at the D1 sampling point, leaf and stem osmotic potential values were still indistinguishable between well-watered and droughted plants (Fig. 3), thereby suggesting that changes in leaf water status and mesophyll cell turgor may not be an absolute requirement for the induction of CAM in *P. oleracea* leaves. This implicates that a signal generated at water-stressed roots may be conveyed to the leaves, where it may promote CAM expression. In

line with this, a split-root experiment conducted with the C_3-CAM facultative species *Mesembryanthemum crystallinum* demonstrated that CAM induction can be triggered before any measurable change in mesophyll cell turgor pressure (Eastmond and Ross, 1997). Although the identity of this endogenous signal remains to be determined in *P. oleracea*, evidence obtained for other facultative CAM species suggests that it may involve the increment in abscisic acid and/or the decline in cytokinin levels (Chu *et al.*, 1990; Dai *et al.*, 1994; Peters *et al.*, 1997; Taybi and Cushman, 2002).

Our findings also indicated that the shift from C_4 to CAM photosynthesis in *P. oleracea* leaves is not part of a preprogrammed developmental process as no evidence of CAM expression was detected in leaves of well-watered plants from the start (D0, 20-day-old, actively-growing plants) to the end of the experiment (R2, 62-day-old, senescing plants). Interestingly, however, whereas the CAM expression in the leaves seem to be exclusively under environmental control, an ontogenetic component in the induction of the CAM pathway may be present in the stems as positive ΔH^+ values and significant *PoPPC2* mRNA accumulation were detected in stems of well-watered plants during the flowering phase (D2 and D3). In line with this, facultative CAM has been interpreted by some authors as an adaptive response that facilitates resource allocation to reproductive structures, thus maximizing reproductive success of annual plants (Herrera, 2009). However, whether the ontogenic induction of CAM in the *P. oleracea* stem has a significant impact on its reproductive output remains to be determined.

Besides assisting in reproductive fitness, CAM may also be interpreted as a strategy to increase water-use efficiency (WUE), minimize photoinhibition and provide photo-protection of the photosynthetic apparatus during prolonged water deficit conditions (Herrera *et al.*, 1991; Herrera, 2009). Monitoring gas exchange and chlorophyll fluorescence revealed that the progressive drought-induced decline in *A*, g_s and *E* were not accompanied by significant changes in F_v/F_m, NPQ and ETR values (Fig. 6), suggesting the daytime decarboxylation of the organic acids accumulated overnight may have supplied CO_2 to Rubisco behind closed stomata at sufficient levels to maintain the photosynthetic apparatus integrity and functioning under drought. Accordingly, very limited changes in C_i/C_a were detected between well-watered and droughted plants, despite the massive decline in *A*, g_s and *E* detected under drought conditions (Fig. 7). Therefore, it seems tempting to suggest that the CAM expression during the drought period may have facilitated the rapid and complete recovery of CO_2 assimilation rates soon after rewatering

by avoiding permanent damages to the photosynthetic apparatus even after prolonged drought exposure. The importance of CAM for photoprotection has also been demonstrated for both constitutive CAM plants and facultative C_3-CAM species (Rascher and Lüttge, 2002; Pikart *et al.*, 2018) and the data presented here seem to be the first indication that a similar process may also take place in facultative C_4-CAM species.

Although nighttime acid accumulation in *P. oleracea* leaves has been shown to depend to some extent on internal refixation of respiratory CO_2, nocturnal CO_2 uptake has also been reported for this species (Winter and Holtum, 2014). In contrast, *P. oleracea* stems are devoid of stomata (Voznesenskaya *et al.*, 2010) therefore, organic acid formation via PEPC in this organ entirely relies on internal refixation of respiratory CO_2. Due to the lack of a typical Kranz anatomy, *P. oleracea* has been regarded as performing C_3 photosynthesis under well-watered conditions (Voznesenskaya *et al.*, 2010). Although anatomical analysis confirmed the absence of typical Kranz anatomy in the stems of both well-watered and droughted plants, it was observed that chloroplasts formed a well-delimited sheath in the inner cortex, surrounding the vascular bundles (Fig. 6). Despite such preferential localization of the chloroplast surrounding the vascular bundles of the stems, which could resemble some features of Kranz-like anatomy, the transcript abundance of C_4-related genes, including *PoCA1*, *PoPPC1* and *PoASPT1*, were drastically lower in stems than in leaves of well-watered plants. Therefore, the data currently available suggest that, depending on the environmental conditions and plant age, *P. oleracea* stems can perform either C_3 or CAM, but not C_4 photosynthesis.

As no conspicuous changes in leaf or stem anatomy were observed after long-term drought exposure (Fig. 5), we can assume that gene expression and biochemical modifications are enough to allow the shift from C_3 (in stems) and C_4 (in leaves) to CAM photosynthesis. Among the changes observed in gene expression during the C_4-to-CAM transition in *P. oleracea* leaves, it is important to highlight that the progressive drought-induced downregulation of C_4-related genes, including *PoCA1*, *PoPPC1* and *PoASPT1*, is concomitant with up-regulation of *PoPPC2* and *PoASPT2*. Conversely, in the stems, not only *PoPPC2* and *PoASPT2*, but also *PoCA3*, *PoMDH4*, *PoNAD-ME1* and *PoNAD-ME2*, are up-regulated in response to drought. These findings have several implications. First, it reveals an opposite influence of water availability on C_4 and CAM machinery, which suggests that either C_4 or CAM, but not both CCMs, can be expressed within the same leaf at the same time. Second, it indicates that among the genes analyzed, the upregulation

of only *PoPPC2* and *PoASPT2* would be required for the CAM functioning in the leaves as the residual activity of other C_4-related enzymes, including those encoded by *PoCA3*, *PoMDH4*, *PoNAD-ME1* and *PoNAD-ME2*, would be sufficient to sustain drought-induced CAM photosynthesis. In contrast, in the C_3-performing tissues of the stems, a more extensive set of components of CAM, including *PoPPC2*, *PoASPT2* as well as CA-, MDH- and ME-encoding genes, needs to be upregulated to sustain the occurrence of the CAM pathway. Third, our findings suggest that the conversion of OAA to aspartate (as well as the reverse reaction) catalyzed by the *PoASPT2*-encoded protein may be a necessary step for the CAM functioning in leaves with typical Kranz anatomy. To the best of our knowledge, this is the first indication that aspartate could be involved in CAM photosynthesis, which needs to be confirmed via additional experimental approaches, including the analysis of ASPT enzymatic activity, the localization of aspartate pools inside the leaves, and monitoring the diel analysis of aspartate fluctuations.

By combining our findings and data from the literature, a highly hypothetical model can be proposed to explain the C_4-CAM functioning in *P. oleracea* leaves (Fig. 16). Immunolocalization experiments conducted in *P. oleracea* leaves indicate that Rubisco is restricted to BSCs whereas PEPC is predominantly found in MCs (Lara *et al.*, 2003). Therefore, under well-watered conditions, the OAA produced via PEPC in the MC during the day would be converted to malate via MDH and/or Asp via ASPT activity. After being shuttled to the BSC, malate may be decarboxylated in the chloroplast via NADP-ME whereas aspartate may be converted to malate in the mitochondria via the coordinated action of ASPT, MDH and subsequently decarboxylated via NAD-ME activity (Fig. 16A). Under drought conditions, a 'C_4-CAM hybrid' system may occur in leaves of droughted *P. oleracea* plants, which involves the nighttime accumulation of organic acids (malate and/or aspartate) in MCs, followed by the transference of these acids to the BSCs during the day. Once in the BSCs, malate and/or aspartate may be decarboxylated, releasing CO_2 close to the active site of Rubisco (Fig. 16B). The pyruvate resulting from the malate decarboxylation may be transported into the chloroplasts of MC chloroplasts, where it is consumed to generate PEP by PPDK. Alternatively, pyruvate can be transaminated to alanine (Ala) by a cytosolic Ala aminotransferase (ALT) before being shuttled to the MC. Inside the MC chloroplast, PEP is used to generate glucose-6-phosphate, which is then used to synthesize starch during the day. Finally, the starch accumulated in the MC chloroplasts can be degraded overnight to regenerate PEP to restart the CAM cycle.

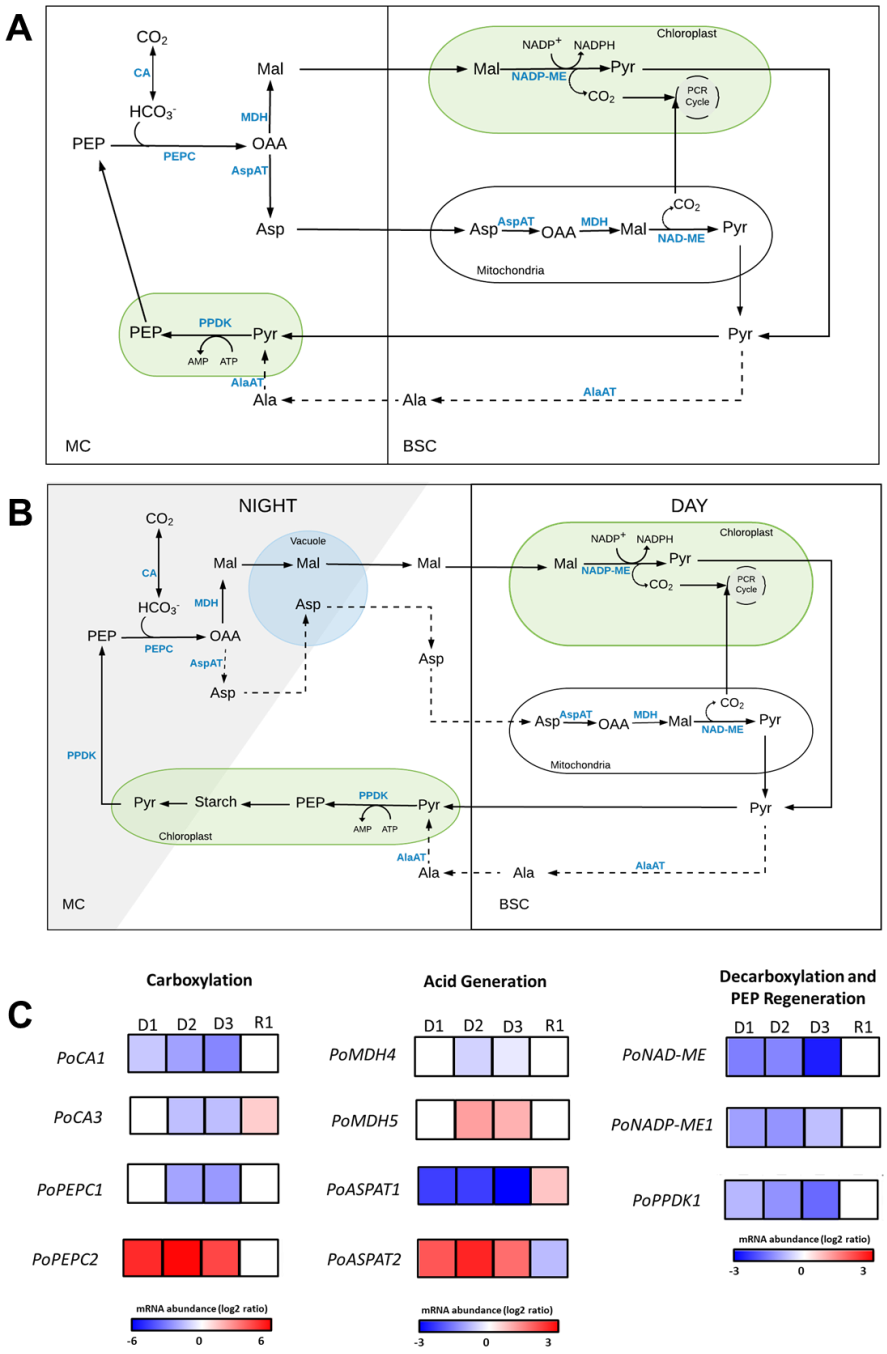

Figure 16: Proposed model summarizing the metabolic reactions potentially involved in the C_4 and CAM pathways in *P. oleracea*. (A) Diagram outlining the reactions potentially required for the C_4 pathway in leaves of well-watered *P. oleracea* plants. **(B)** Schematic representation of the reactions potentially required for the 'C_4-CAM hybrid' pathway in leaves of droughted *P. oleracea* plants. **(C)** Heatmap representing the statistically significant differences in mRNA levels of C_4- and CAM- related genes compared to the drought samples (Student's t-test, $P<0.05$). Key metabolites include: PEP, phospho*enol*pyruvate; OAA, oxaloacetate; Mal, malate; Asp, aspartate; Pyr, pyruvate; Ala, Alanine. Key enzymes include: CA, carbonic anhydrase; PEPC, PEP carboxylase; MDH, malate dehydrogenase; AspAT,

aspartate aminotransferase; NAD-ME, NAD-malic enzyme; NADP-ME, NADP-malic enzyme; AlaAT, alanine aminotransferase; PPDK, pyruvate phosphate dikinase. In B, the gray area indicates reaction taking place in the nighttime. Chloroplasts, vacuoles and mitochondria are represented in green, blue and yellow, respectively. Dashed arrows represent alternative pathways.

It is important to highlight that the model here proposed is highly hypothetical. For example, the suggestion that both malate and aspartate may play a role as transfer acid is exclusively based on the drought-induced fluctuation in mRNA levels of genes encoding enzymes responsible for producing these acids (Fig. 16C). However, in line with our findings, accumulating evidence indicates that C_4 plants tend to use a combination of transfer acids and decarboxylation systems, which may provide adaptive advantages by facilitating the adjustment of the energy balance between MC and BSC in response to changes in the environmental conditions (Wang *et al.*, 2014; Ludwig, 2016). Therefore, additional investigation is needed to clarify whether *P. oleracea* uses a combination of transferred organic acids and carboxylases when performing either C_4 or the 'C_4-CAM hybrid' pathways.

6. Conclusion and Future Remarks

Altogether, our findings reveal a remarkable photosynthetic plasticity in *P. oleracea* and start to elucidate the key components responsible for the compatibility between the C_4 and CAM pathway in this species. CAM was shown to be expressed in a fully facultative fashion in leaves, whereas both ontogenetic and environmental cues seem to control the induction of this photosynthetic behavior in stem tissues. Gas exchange and chlorophyll *a* fluorescence analysis in droughted plants suggested that the daytime decarboxylation of the organic acids accumulated overnight may have supplied CO_2 to Rubisco behind closed stomata at sufficient levels to maintain the photosynthetic apparatus integrity and functioning even after prolonged drought exposure. Overall, no marked anatomical changes were observed in leaves or stems during the CAM induction, suggesting that gene expression and metabolism reprogramming may account for most of the C_4-to-CAM and C_3-to-CAM transition in leaves and stems, respectively. Transcriptional data indicated that distinct *PPC* and *ASPT* genes were recruited to allow C_4 and CAM compatibility within a single leaf. Gene expression evidence also indicated that the switch between C_3 and CAM pathways in the stems requires the transcriptional regulation of a more extensive set of CCM-related genes than the C_4-to-CAM transition in the leaves.

Taking into account these results, this study also raises important questions for future investigations, such as:

Where are the key components of the 'C_4-CAM hybrid' pathway localized within the cells and tissues?

Answering this question will require further experiments characterizing the intra-cellular and tissue distribution of enzymes responsible for the major C_4/CAM-related reactions (e.g., PEPC, ASPT, ME, MDH, PPDK). A combination of approaches including *in situ* hybridization, tissue immunolocalization, laser microdissection RNAseq (LM-RNAseq), as well as promoter-reporter and protein-reporter fusion assays, may be required to adequately determine the intra-cellular and tissue localization of the individual components of this 'C_4-CAM hybrid' pathway.

Are multiple transfer organic acids and decarboxylation systems involved in the 'C_4-CAM hybrid' pathway?

Monitoring the diel fluctuations in metabolites as well as the activities of C_4/CAM-related enzymes may be instrumental for answering this question. Dissecting whether malate and/or

aspartate play a significant role as transfer acids in the 'C_4-CAM hybrid' pathway, and determining the relative contribution of NAD-ME, NADP-ME and PEP carboxykinase (PEPCK) as the decarboxylation system in *P. oleracea* BSC may provide valuable insights into the functioning of CAM in a leaf exhibiting typical dual-cell C_4 anatomy.

How many genes should be manipulated to engineer CAM into C_4 species?

Among the genes analyzed in this study, only *PoPPC2* and *PoASPT2* were sharply up-regulated to sustain the 'C_4-CAM hybrid' pathway in leaves of droughted *P. oleracea* plants. Therefore, one could argue that perhaps a relatively limited number of genetic manipulations may be required to engineer CAM into C_4 leaves. However, it is important to highlight that a relatively small number of genes were analyzed in this study; therefore, future studies exploring other core C_4/CAM genes as well as accessory pathways (e.g., sugar metabolism, stomatal control) may provide a more comprehensive list of candidate genes for future attempts of engineering facultative CAM into C_4 crop species.

What are the adaptive advantages of facultative CAM for a C_4 plant?

Perhaps the best strategy to answer this fundamental question involves generating CAM-deficient *P. oleracea* mutants or transgenics. In this context, knockout/knockdown of *PoPPC2* and *PoASPT2* seem to be a promising venue to achieve CAM-deficient *P. oleracea* plants, whose development, metabolism and reproductive success under stressful conditions could be compared to wild-type counterparts. The use of organ-specific promoters for the generation of the knockdown lines may also facilitate dissecting the adaptive relevance of the CAM photosynthesis in *P. oleracea* leaves and stems.

We hope the findings presented in this Dissertation substantiate further advances in understanding the C_4/CAM compatibility within a single individual, thereby instigating future attempts to incorporate facultative CAM-like traits into C_4 crop species via synthetic biology and other biotechnological tools.

7. References

Aubry S, Brown NJ, Hibberd JM. 2011. The role of proteins in C_3 plants prior to their recruitment into the C_4 pathway. Journal of Experimental Botany **62**, 3049–3059.

Badger MR, Price GD. 1994. The role of carbonic anhydrase in photosynthesis. Plant physiology and plant molecular biology **45**, 369–392.

Bauwe H, Hagemann M, Fernie AR. 2010. Photorespiration: players, partners and origin. Trends in Plant Science **15**, 330–336.

Brautigam A, Kajala K, Wullenweber J, *et al.* 2011. An mRNA blueprint for C_4 photosynthesis derived from comparative transcriptomics of closely related C_3 and C_4 species. Plant Physiology **155**, 142–156.

Bräutigam A, Schliesky S, Külahoglu C, Osborne CP, Weber APM. 2014. Towards an integrative model of C_4 photosynthetic subtypes: insights from comparative transcriptome analysis of NAD-ME, NADP-ME, and PEPCK C_4 species. Journal of Experimental Botany **65**, 3579–3593.

Chastain CJ, Failing CJ, Manandhar L, Zimmerman MA, Lakner MM, Nguyen THT. 2011. Functional evolution of C_4 pyruvate, orthophosphate dikinase. Journal of Experimental Botany **62**, 3083–3091.

Christin PA, Arakaki M, Osborne CP, *et al.* 2014. Shared origins of a key enzyme during the evolution of C_4 and CAM metabolism. Journal of Experimental Botany **65**, 3609–3621.

Chu C, Dai Z, Ku MSB, Edwards GE. 1990. Induction of Crassulacean acid metabolism in the facultative halophyte *Mesembryanthemum crystallinum* by abscisic acid. Plant Physiology **93**, 1253–1260.

Cushman JC. 2001. Crassulacean acid metabolism. A plastic photosynthetic adaptation to arid environments. American Society of Plant Biologists **127**, 1439–1448.

Cushman JC, Borland AM. 2002. Induction of Crassulacean acid metabolism by water limitation. Plant, Cell and Environment **25**, 295–310.

Dai Z, Ku MSB, Zhang D, Edwards GE. 1994. Effects of growth regulators on the induction of Crassulacean acid metabolism in the facultative halophyte *Mesembryanthemum crystallinum* L. Planta **192**, 287–294.

Eastmond PJ, Ross JD. 1997. Evidence that the induction of crassulacean acid

metabolism by water stress in *Mesembryanthemum crystallinum* (L.) involves root signalling. Plant, Cell and Environment **20**, 1559–1565.

Edwards GE, Franceschi VR, Voznesenskaya E V. 2004. Single-Cell C_4 photosynthesis versus the dual-cell (Kranz) paradigm. Annual Review of Plant Biology **55**, 173–196.

Edwards EJ, Ogburn RM. 2012. Angiosperm responses to a low-CO_2 World: CAM and C_4 photosynthesis as parallel evolutionary trajectories. International Journal of Plant Sciences **173**, 724–733.

Edwards EJ, Osborne CP, Stromberg CAE, *et al.* 2010. The origins of C_4 grasslands: integrating evolutionary and ecosystem science. Science **328**, 587–591.

Freitag H, Stichler W. 2000. A remarkable new leaf type with unusual photosynthetic tissue in a central Asiatic genus of Chenopodiaceae. Plant Biology **2**, 154–160.

Freschi L, Rodrigues MA, Domingues DS, Purgatto E, Sluys M Van, Magalhaes JR, Kaiser WM, Mercier H. 2010. Nitric oxide mediates the hormonal control of Crassulacean acid metabolism expression in young pineapple plants. Plant Physiology **152**, 1971–1985.

Furbank RT. 2011. Evolution of the C_4 photosynthetic mechanism: are there really three C_4 acid decarboxylation types? Journal of Experimental Botany **62**, 3103–3108.

Guralnick LJ, Edwards G, Ku MSB, Hockema B, Franceschi VR. 2002. Photosynthetic and anatomical characteristics in the C_4–crassulacean acid metabolism-cycling plant, Portulaca grandiflora. **29**.

Guralnick LJ, Jackson MD. 2001. The occurrence and phylogenetics of Crassulacean acid metabolism in the Portulacaceae. International Journal **162**, 257–262.

Hatch MD, Agostino A, Burnell JN. 1988. Photosynthesis in phosphoenolpyruvate carboxykinase-type C_4 plants: Activity and role of mitochondria in bundle sheath cells. Archives of Biochemistry and Biophysics **261**, 357–367.

Herrera A. 2009. Crassulacean acid metabolism and fitness under water deficit stress: If not for carbon gain, what is facultative CAM good for? Annals of Botany **103**, 645–653.

Herrera A, Delgado J, Paraguatey I. 1991. Occurrence of inducible Crassulacean acid metabolism in leaves of *Talimum triangulare* (Portulacaceae). Journal of Experimental Botany **42**, 493–499.

Holtum JAM, Aranda J, Virgo A, Gehrig HH, Winter K. 2004. δ13C values and

crassulacean acid metabolism in *Clusia* species from Panama. Trees - Structure and Function **18**, 658–668.

Holtum JAM, Hancock LP, Edwards EJ, Winter K. 2017. Optional use of CAM photosynthesis in two C_4 species, *Portulaca cyclophylla* and *Portulaca digyna*. Journal of Plant Physiology **214**, 91–96.

Holtum JAM, Hancock LP, Edwards EJ, Winter K. 2018. Crassulacean acid metabolism (CAM) in the Basellaceae (Caryophyllales). ARPN Journal of Engineering and Applied Sciences **12**, 3218–3221.

Kadereit G, Borsch T, Weising K, Freitag H. 2013. Phylogeny of Amaranthaceae and Chenopodiaceae and the evolution of C_4 photosynthesis. International Journal of Plant Sciences **164**, 959–986.

Kanai R., Edwards GE. 1999. The biochemistry of C_4 photosynthesis. Biochemistry, 3–6.

Koch KE, Kennedy RA. 1980. Characteristics of Crassulacean *Acid Metabolism in the Succulent* C_4 dicot, *Portulaca oleracea* L. Plant Physiology **65**, 193–197.

Koch K, Kennedy R. 1982. Crassulacean acid metabolism in the succulent C_4 dicot, *Portulaca oleracea* L under natural environmental conditions. Plant Physiology **69**, 757–761.

Kraybill AA, Martin CE. 1996. Crassulacean acid metabolism in three species of the C_4 Genus *Portulaca*. International Journal of Plant Sciences **157**, 103–109.

Ku SB, Shieh YJ, Reger BJ, Black CC. 1981. Photosynthetic characteristics of *Portulaca grandiflora*, a succulent C_4 dicot. Plant Physiology **68**, 1073–1080.

Lara M V., Disante KB, Podestá FE, Andreo CS, Drincovich MF. 2003. Induction of a Crassulacean acid like metabolism in the C_4 succulent plant, *Portulaca oleracea* L.: Physiological and morphological changes are accompanied by specific modifications in phosphoenolpyruvate carboxylase. Photosynthesis Research **77**, 241–254.

Lara M V., Drincovich MF, Andreo CS. 2004. Induction of a crassulacean acid-like metabolism in the C4 succulent plant, *Portulaca oleracea* L.: Study of enzymes involved in carbon fixation and carbohydrate metabolism. Plant and Cell Physiology **45**, 618–626.

Livak KJ, Schmittgen TD. 2001. Analysis of relative gene expression data using real-time quantitative PCR and the 2-ΔΔCT method. Methods **25**, 402–408.

Long JJ, Wang JL, Berry JO. 1994. Cloning and analysis of the C_4-photosynthetic

NAD-dependent malic enzyme of amaranth mitochondria. Journal of Biological Chemistry **269**, 2827–2833.

Ludwig M. 2016. The roles of organic acids in C_4 photosynthesis. Frontiers in Plant Science **7**, 1–11.

Lüttge U. 2004. Ecophysiology of Crassulacean acid metabolism (CAM). Annals of Botany **93**, 629–652.

Lüttge U. 2006. Photosynthetic flexibility and ecophysiological plasticity: Questions and lessons from *Clusia*, the only CAM tree, in the neotropics. New Phytologist **171**, 7–25.

Martin CE, Zee a K. 1983. C_3 photosynthesis and crassulacean acid metabolism in a Kansas rock outcrop succulent, *Talinum calycinum* Engelm. (Portulacaceae). Plant Physiology **73**, 718–723.

Maxwell K, Johnson GN. 2000. Chlorophyll fluorescence - a practical guide. Journal of Experimental Botany **51**, 659–668.

Mazen AMA. 1996. Changes in properties of phosphoenolpyruvate carboxylase with induction of Crassulacean Acid Metabolism (CAM) in the C_4 plant *Portulaca oleracea*. Photosynthetica **38**, 385–391.

Mazen AMA. 2000. Changes in levels of phosphoenolpyruvate carboxylase with induction of Crassulacean acid metabolism (CAM) like behavior in the C_4 plant *Portulaca oleracea*. Physiol Plant **98**, 111–116.

McKown AD, Moncalvo JM, Dengler NG. 2005. Phylogeny of *Flaveria* (Asteraceae) and inference of C_4 photosynthesis evolution. American Journal of Botany **92**, 1911–1928.

Medina E, Delgado M, Troughton JH, Medina JD. 1977. Physiological ecology of CO_2 fixation in Bromeliaceae. Flora **166**, 137–152.

Muhaidat R, Sage RF, Dengler NG. 2007. Diversity of Kranz anatomy and biochemistry in C_4 eudicots. American Journal of Botany **94**, 362–381.

Ocampo G, Koteyeva NK, Voznesenskaya E V., Edwards GE, Sage TL, Sage RF, Travis Columbus J. 2013. Evolution of leaf anatomy and photosynthetic pathways in Portulacaceae. American Journal of Botany **100**, 2388–2402.

Osborne CP, Sack L. 2012. Evolution of C_4 plants: a new hypothesis for an interaction of CO_2 and water relations mediated by plant hydraulics. Philosophical Transactions of the Royal Society B: Biological Sciences **367**, 583–600.

Peterhansel C, Maurino VG. 2011. Photorespiration redesigned. Plant Physiology **155**, 49–55.

Peters W, Beck E, Piepenbrock M, Lenz B, Schmitt JM. 1997. Cytokinin as a negative effector of phosphoenolpyruvate carboxylase induction in *Mesembryanthemum crystallinum*. Journal of Plant Physiology **151**, 362–367.

Pikart FC, Marabesi MA, Mioto PT, Gonçalves AZ, Matiz A, Alves FRR, Mercier H, Aidar MPM. 2018. The contribution of weak CAM to the photosynthetic metabolic activities of a bromeliad species under water deficit. Plant Physiology and Biochemistry **123**, 297–303.

Rascher U, Lüttge U. 2002. High-resolution chlorophyll fluorescence imaging serves as a non-invasive indicator to monitor the spatio-temporal variations of metabolism during the day-night cycle and during the endogenous rhythm in continuous light. Plant Biology **4**, 671–681.

Raven JA, Beardall J. 2016. The ins and outs of CO_2. Journal of Experimental Botany **67**, 1–13.

Sage RF. 2002. Are Crassulacean acid metabolism and C_4 photosynthesis incompatible? Functional Plant Biology **29**, 775–785.

Sage RF. 2004. The evolution of C_4 photosynthesis. New Phytologist **161**, 341–370.

Sage RF, Christin P-A, Edwards EJ. 2011. The C_4 plant lineages of planet Earth. Journal of Experimental Botany **62**, 3155–3169.

Sage RF, Khoshravesh R, Sage TL. 2014. From proto-Kranz to C_4 Kranz: building the bridge to C_4 photosynthesis. Journal of Experimental Botany **65**, 3341–3356.

Sage RF, Sage TL, Kocacinar F. 2012. Photorespiration and the evolution of C_4 photosynthesis. Annual Review of Plant Biology **63**, 19–47.

Santa-Cruz A, Martinez-Rodriguez MM, Perez-Alfocea F, Romero-Aranda R, Bolarin MC. 2002. The rootstock effect on the tomato salinity response depends on the shoot genotype. Plant Science **162**, 825–831.

Silvera K, Kurt MN, Mark Whitten W, Williams NH., Winter K, Cushman JC. 2010. Evolution along the crassulacean acid metabolism continuum. Functional Plant Biology **37**, 995–1010.

Taybi T, Cushman JC. 2002. Abscisic acid signaling and protein synthesis requirements for phosphoenolpyruvate carboxylase transcript induction in the common ice plant. Journal of Plant Physiology **159**, 1235–1243.

Vieira EA, da Cruz Centeno D, Freschi L, da Silva EA, Braga MR. 2017. The dual strategy of the bromeliad *Pitcairnia burchellii* Mez to cope with desiccation. Environmental and Experimental Botany **143**, 135–148.

Vogan PJ, Frohlich MW, Sage RF. 2007. The functional significance of C_3-C_4 intermediate traits in *Heliotropium* L. (Boraginaceae): Gas exchange perspectives. Plant, Cell and Environment **30**, 1337–1345.

Voznesenskaya E V, Franceschi VR, Kiirats O, Artyusheva EG, Freitag H, Edwards GE. 2002. Proof of C_4 photosynthesis without Kranz anatomy in *Bienertia cycloptera* (Chenopodiaceae). Plant Journal **31**, 649–662.

Voznesenskaya E V., Koteyeva NK, Edwards GE, Ocampo G. 2010. Revealing diversity in structural and biochemical forms of C_4 photosynthesis and a C_3-C_4 intermediate in genus *Portulaca* L. (Portulacaceae). Journal of Experimental Botany **61**, 3647–3662.

Voznesenskaya E V., Koteyeva NK, Edwards GE, Ocampo G. 2017. Unique photosynthetic phenotypes in *Portulaca* (Portulacaceae): C_3-C_4 intermediates and NAD-ME C_4 species with Pilosoid-type Kranz anatomy. Journal of Experimental Botany **68**, 225–239.

Wang Y, Bräutigam A, Weber APM, Zhu XG. 2014. Three distinct biochemical subtypes of C_4 photosynthesis? A modelling analysis. Journal of Experimental Botany **65**, 3567–3578.

Whitney SM, Houtz RL, Alonso H. 2011. Advancing our understanding and capacity to engineer nature's CO_2-sequestering enzyme, Rubisco. Plant Physiology **155**, 27–35.

Winter K, Garcia M, Holtum JAM. 2008. On the nature of facultative and constitutive CAM: Environmental and developmental control of CAM expression during early growth of *Clusia, Kalanchoë,* and *Opuntia*. Journal of Experimental Botany **59**, 1829–1840.

Winter K, Garcia M, Holtum JAM. 2009. Canopy CO_2 exchange of two neotropical tree species exhibiting constitutive and facultative CAM photosynthesis, *Clusia rosea* and *Clusia cylindrica*. Journal of Experimental Botany **60**, 3167–3177.

Winter K, Holtum JAM. 2002. How closely do the d13 C values of Crassulacean acid metabolism plants reflect the proportion of CO_2 fixed during day and night? Plant Physiology **129**, 1843–1851.

Winter K, Holtum JAM. 2011. Induction and reversal of crassulacean acid metabolism in *Calandrinia polyandra*: Effects of soil moisture and nutrients. Functional Plant Biology **38**,

576–582.

Winter K, Holtum JAM. 2014. Facultative crassulacean acid metabolism (CAM) plants: Powerful tools for unravelling the functional elements of CAM photosynthesis. Journal of Experimental Botany **65**, 3425–3441.

Winter K, Holtum JAM. 2017. Facultative crassulacean acid metabolism (CAM) in four small C_3 and C_4 leaf-succulents. Australian Journal of Botany **65**, 103.

Zhang YG, Pagani M, Liu Z, *et al.* 2013. A 40-million-year history of atmospheric CO_2 A 40-million-year history of atmospheric CO_2. Royal Society **371**, 20130096.